Title: Cyclometallation, Steric and Electronic Tendencies In a Series of Pd(II) Complex Pre-catalysts Bearing Imidazole-phenol Ligands and Effects on Suzuki-Miyaura Catalytic Efficiencies

Author: Abiodun O. Eseola Helmar Gorls Joseph A.O. Woods Winfried Plass

PII: S1381-1169(15)00212-5
DOI: http://dx.doi.org/doi:10.1016/j.molcata.2015.06.001
Reference: MOLCAA 9514

To appear in: *Journal of Molecular Catalysis A: Chemical*

Received date: 19-3-2015
Revised date: 30-5-2015
Accepted date: 1-6-2015

Please cite this article as: Abiodun O.Eseola, Helmar Gorls, Joseph A.O.Woods, Winfried Plass, Cyclometallation, Steric and Electronic Tendencies In a Series of Pd(II) Complex Pre-catalysts Bearing Imidazole-phenol Ligands and Effects on Suzuki-Miyaura Catalytic Efficiencies, Journal of Molecular Catalysis A: Chemical http://dx.doi.org/10.1016/j.molcata.2015.06.001

Cyclometallation, Steric and Electronic Tendencies In a Series of Pd(II) Complex Pre-catalysts Bearing Imidazole-phenol Ligands and Effects on Suzuki-Miyaura Catalytic Efficiencies

Abiodun O. Eseola[§,‡*] bioduneseola@hotmail.com bioduneseola@run.edu.ng, Helmar Gorls[‡], Joseph A. O. Woods[II], Winfried Plass[‡]*sekr.plass@uni-jena.de
[§]Materials Chemistry Group, Department of Chemical Sciences, Redeemer's University, Redemption City, Ogun State, Nigeria.
[‡]Institut für Anorganische und Analytische Chemie, Friedrich-Schiller-Universität Jena, Humboldtstr. 8, D-07743 Jena, Germany.
[II]Inorganic Chemistry Unit, Department of Chemistry, University of Ibadan, Ibadan – Nigeria.
[*]Corresponding author. Tel.: +234(0)7062192104 (Abiodun O. Eseola); Tel.: +49 3641 948130;

Fax: +49 3641948132 (Winfried Plass).

Graphical Abstract

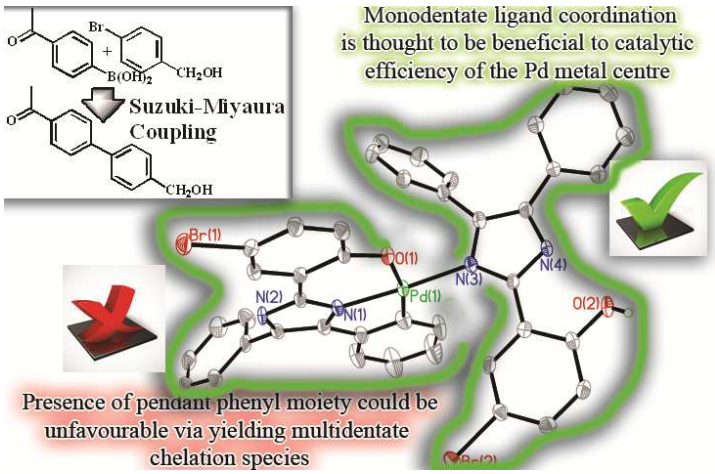

Highlights

- Structural evidences were obtained for unfavourable cyclometallation of phenyls.
- Ligand substituent electronic effects seem to affect cyclometallation tendency.
- Results suggest that cyclometallation caused poor catalytic prospects.
- Ligands with hemilabile or sterically distorted donors gave good catalytic outcome.
- Bulky ligand framework is not a necessity for high coupling efficiency.
- Catalyst developers should avoid coordinating carbons in the vicinity of palladium.

Highlights

- Structural evidences were obtained for cyclometallation of nearby phenyls to Pd^{II}.
- Results suggest that cyclometallation largely cut down catalytic prospects.
- Electronic effects of ligand substituents seem to affect cyclometallation tendency.
- Bidentate ligands with hemilabile or sterically hindered donors are beneficial.
- Bulky ligand framework is seen not to be a necessity for high coupling efficiency.

Abstract

A series of new structurally and electronically diversified palladium complexes derived from seven less sterically crowded 2-(4,5-dimethyl-1H-imidazol-2-yl)phenol / 2-(4,5-diethyl-1H-imidazol-2-yl)phenol ligands and fourteen 2-(4,5-diphenyl-1H-imidazol-2-yl)phenols / 2-(1H-phenanthro[9,10-d]imidazol-2-yl)phenols bearing varying degrees of higher steric bulk have been prepared and characterized. While single crystals grown from precipitated products of complexation reactions confirmed the bis-ligand **Pd(N^O)$_2$** coordination, few crystals obtained from reaction filtrates involving the 2-(4,5-diphenyl-1H-imidazol-2-yl)phenols provided evidence for formation of N^O^C chelation species achieved by cyclometallation. Results from structural analyses and catalytic outcomes generally indicate that desirable variables on the ligand frameworks for obtaining superior catalyst activities either provides hemilabile or sterically strained chelation characters, which would both favour generation of monodentate coordination species at the catalysis temperature. In particular, correlation was observed between tendency for cyclometallation in the palladium complexes and poor Suzuki-Miyaura catalytic prospects. Based on hopeful activity obtained for the complex bearing 4-bromo-2-(4,5-dimethyl-1H-imidazol-2-yl)phenol, it was also concluded that sterically bulky ligand is not a necessity for high coupling efficiency, while presence of potentially cyclometallating substituent moieties in the vicinity of the palladium centre may in fact destroy catalytic prospects.

Keywords: Organometallic cyclometallation; palladacycle; Homogeneous catalysis; Structure-Property Correlation; Suzuki-Miyaura coupling

Introduction

In the past few decades, palladium compounds have been keenly investigated and respected for their versatile catalytic roles in synthetic molecular sciences. They provide cheap and seamless catalytic access to many C-C coupling reactions, which were either only imagined or too expensive to achieve in terms of time, multi-step reactions involved and resources.[1-8] Therefore, industrial and academic research fields concerned with rigorous organic synthetic manipulations such as in drug design, natural product total synthesis, synthetic materials sciences and supramolecular architectural designs have come to recognize Pd-catalyzed C-C coupling strategies as invaluable molecular building tools.[9-18] Some notably efficient catalytic compounds have already been commercialized; e.g. PEPPSI™.[19] Suzuki-Miyaura reaction, which is the direct cross-coupling of an aryl halide with boron-containing reagents in the presence of palladium catalyst, is arguably one of the easiest and most widely applied C-C cross-coupling method.[20-26]

Numerous forms of palladium species have been studied as pre-catalysts for Suzuki-Miyaura cross-coupling and nearly all reported forms of palladium materials such as soluble ligand-free palladium species, discrete soluble palladium complexes, palladium-exchanged oxides, palladium nano- and macro-particles, etc., have been presented as potentially highly active catalyst species.[27] Hence, the true homogeneous / heterogeneous nature of the active species has continued to be a subject of debate.[27-32] For instance, while some recent reports suggested that unprecedented catalyst performance was encountered for soluble Pd(0) species bearing monodentate ligands with sterically bulky side arms,[5,31] other views believe that high activities would be obtained with ligandless palladium species.[29-30] Hence, despite decades of investigations on Pd-catalyzed C-C cross-coupling catalysis, research activities have continued

to generate contributions aimed at improving the understanding of the role of the various forms of palladium species in C-C coupling catalysis. Recent research outputs have progressively narrowed down on palladium species that could be considered to possess superior activity.

Homogeneous catalytic examination of rationally structured series of complexes is an important means towards improving the understanding of the catalyst active site configurations. Such depth of study is less possible with heterogeneously supported catalysis due to less defined knowledge of molecular-level characteristics for surface supported materials among other set-becks.[33-37] Moreover, investigations involving reasonable number of palladium complex pre-catalysts derived from ligands with known and systematically varied electronic donor trends / steric directionalities is scarce.[26,34,38,39,40]

In recent studies, experimental donor strength determinations coupled with DFT calculations revealed that our library of 2-(1H-imidazol/oxazol-2-yl)phenols and 2-(1H-imidazol/oxazol-2-yl)pyridines are hemilabile such that, while the phenolic oxygen-donor atoms or pyridyl nitrogen have fairly good donor characteristics, donor strengths of the imidazole / ozazole arm of the bidentate ligands could be varied from very poorly donating to fairly strongly donating. Furthermore, the azole donor strengths were observed to be influenced by the nature of substituents directly bonded to the azole rings as well as on those remotely located on the 2-aryl-substituent of the azole ring. In particular, oxazole moieties in these ligand families were observed to be poorer donors compared to imidazoles.[41-45] On the basis of knowledge derived from observed structural results of some members of the 2-(1H-imidazol-2-yl)phenol series[39,46] and donor strength studies[42,43,45,47] conducted for the ligand family, it was anticipated that a relatively wide variations in coordination / chelation preference would exist for palladium complexes of the 2-(1H-imidazol-2-yl)phenols. Furthermore, it was anticipated that, with

systematic variation on ligand electronic, steric and chelation characters, some information about the configuration of active palladium species would be learned.

Consequently, the aims of this study are to rationally synthesize and characterize more of the 2-(1H-imidazol-2-yl)phenol series, prepare their corresponding palladium(II) complex pre-catalysts and to study the dependence of their Suzuki-Miyaura coupling efficiencies on the coordinated ligand frameworks (**Scheme 1(a) – (c)**). We herein present the results for synthesis, characterization and catalytic performance of a new series of palladium(II) complexes derived from structurally and electronically diverse ligand frameworks (**Scheme 1**). On the basis of X-ray crystal structures of palladium species that crystallized from the filtrates of some complexation reactions, the observed cyclometallation tendency of the 4,5-diphenyl-imidazolyl ligand analogues and its poisoning implication on catalytic efficiency is also discussed.

Experimental

General Information

All starting materials for syntheses as well as substrates for catalytic experiments were obtained commercially as reagent grade and used as supplied. The compounds ***p*-*t*Bu~dm**, ***p*-M~dm**, ***p*-N~dm**, **de**, ***o*-*t*Bu~dp**, **dp**, ***o*-H~dp**, ***o*-M~dp**, ***p*-M~dp**, ***p*-Br~dp**, ***p*-N~dp**, **Naph~dp**, ***m*-M~pt**, **Bis-Im**, **Pd(*p*-N~dm)$_2$** and **Pd(de)$_2$** were obtained according to recently reported procedures.[39,42,45,46] In order to exclude impurities, the organic compounds were either purified on silica gel columns or re-crystallized. Elemental analyses were performed on Leco CHNS-932 or El Vario III elemental analyzers. ^{1}H and ^{13}C NMR spectra were recorded on Bruker ARX 200 or 400 MHz instrument using deuterated solvents and TMS as internal standard. IR spectra were recorded on Shimadzu 8740 FT-IR spectrometer as KBr discs in the range of 4000–400 cm^{-1}.

Single crystal X-ray analyses were carried out on a Nonius Kappa CCD diffractometer at 133(2) K using graphite monochromated Mo-Kα radiation (k = 0.71073 Å). Cell parameters were obtained by global refinement of the positions for all collected reflections. The structures were solved by direct methods and refined by full-matrix least-squares on F2. All non-hydrogen atoms were refined anisotropically. The protons on the imidazole rings were picked on the difference maps during structure refinement, which confirms the azole rings are not oxazoles. Structure solutions and refinements were performed using the *SHELX-97* package.[48]

Preparation of 2-(1H-Imidazol-2-yl)phenol Ligands

2-*Tert*-butyl-6-(4,5-dimethyl-1H-imidazol-2-yl)phenol (*o*-*t*Bu~dm): 3-tert-butyl-2-hydroxybenzaldehyde (1.78 g, 10.00 mmol), butane-2,3-dione (0.86 g, 10.00 mmol) and ammonium acetate (≈10 g, 129.73 mmol) were weighed in to a round bottomed flask and refluxed for 3 hours after addition of ≈ 10 mL ethanol and in the presence of ≈ 0.5 mL glacial acetic acid as catalyst. The resulting reaction solution was cooled, diluted with distilled water (≈ 30 mL), neutralized by concentrated ammonia solution and the crude product was extracted with dichloromethane, concentrated and purified on silica gel column using ethyl acetate / n-hexane (1:5) as eluent. The product obtained from chromatography was recrystallyzed from ethanol to obtain ***o*-*t*Bu~dm** (1.05 g, 47 %). Mp. 112-113 ^{o}C. Selected IR peaks (KBr, cm^{-1}): ν 3462vs(vsh), 3397s, 2947s, 1614vs, 1595m, 1447vs, 740s. ^{1}H NMR (200 MHz, TMS, d_6-dmso); δ_{ppm} 13.83 (s, 1H); 12.27 (s, 1H), 7.60 (d, *J* = 7.8 Hz, 1H, phenol ring); 7.12 (d, *J* = 7.6 Hz, 1H, phenol ring); 6.78 (dd, *J* = 7.8 Hz, 1H, phenol ring); 2.20 (s, 3H, methyl); 2.12 (s, 3H, methyl); 1.39 (s, 9H, *t*-Bu). ^{13}C NMR (50 MHz, d_6-dmso): 155.22, 143.91, 136.27, 129.43, 125.62, 121.82, 117.73,

113.28, 34.44, 29.23. Anal. Calc. for $C_{15}H_{20}N_2O^{\cdot 1}/_7$EtOH: C, 73.24; H, 8.36; N, 11.20 %. Found: C, 73.15; H, 8.36; N, 11.20 %.

2-Methoxy-6-(4,5-dimethyl-1H-imidazol-2-yl)phenol (*o*-M~dm): 2-hydroxy-3-methoxybenzaldehyde (1.52 g, 10.00 mmol), butane-2,3-dione (0.86 g, 10.00 mmol) and ammonium acetate (≈ 10 g, 129.73 mmol) were refluxed for 2 hours in ethanol (15 mL) in the presence of catalytic amount of glacial acetic acid. The resulting reaction solution was cooled, diluted with water (≈ 30 mL), carefully neutralized with aqueous ammonia and extracted with dichloromethane (≈ 50 mL twice). The organic extract was concentrated and purified on silica gel column using ethyl acetate / n-hexane (1:4) as eluent to obtain ***o*-M~dm** (0.09 g, 4 %). Mp. 234-244 ^{o}C. Selected IR peaks (KBr, cm^{-1}): ν 3339vs(sh), 3015w, 2922m, 1616s, 735s. ^{1}H NMR (400 MHz, TMS, d_6-dmso); δ_{ppm} 13.20 (s, 1H); 12.29 (s, 1H); 7.33 (d, *J* = 7.6 Hz, 1H, phenol ring); 6.87 (d, *J* = 8.0 Hz, 1H, phenol ring); 6.80 (dd, *J* = 8.0 Hz, 1H, phenol ring); 3.77 (s, 3H, methoxy); 2.17 (s, 3H); 2.13 (s, 3H). ^{13}C NMR (100 MHz, d_6-dmso): 148.27; 146.32, 143.52, 118.13, 115.64, 113.44, 111.75, 55.57 (methoxy), 11.7. MS (EI) m/z 218 (M^+, 100 %): 218, 200, 188, 175, 28. Anal. Calc. for $C_{12}H_{14}N_2O_2$.: C, 65.81; H, 6.37; N, 11.81 %. Found: C, 66.05; H, 6.44; N, 11.50 %.

4-Bromo-2-(4,5-dimethyl-1H-imidazol-2-yl)phenol (*p*-Br~dm): 5-bromo-2-hydroxybenzaldehyde, (2.01 g, 10.00 mmol), butane-2,3-dione (0.86 g, 10.00 mmol) and ammonium acetate (≈10 g, 129.73 mmol) were reacted and purified in similar manner as for preparation of ***o*-*t*Bu~dm** above to obtain ***p*-Br~dm** (0.60 g, 23 %). Mp. 257-258 ^{o}C. Selected IR peaks (KBr, cm^{-1}): ν 3327s(sh), 2922m, 1618s, 1580s, 805s. ^{1}H NMR (200 MHz, TMS, d_6-

dmso); δ_{ppm} 13.10 (s, 1H); 12.57 (s, 1H); 7.96 (d, *J* = 2.4 Hz, 1H, phenol ring); 7.29 (dd, *J* = 2.4, 8.8 Hz, 1H, phenol ring); 6.85 (d, *J* = 8.6 Hz, 1H, phenol ring); 2.15 (s, 6H, 4,5-dimethyl). ^{13}C NMR (50 MHz, d_6-/): 155.39, 141.86, 131.17, 125.84, 118.77, 115.35, 109.69. MS (EI) m/z 267 (M^+, 100 %): 267, 187, 159, 42. Anal. Calc. for $C_{11}H_{11}BrN_2O$: C, 49.46; H, 4.15; N, 10.49 %. Found: C, 49.78; H, 3.94; N, 10.46 %.

4-*Tert*-butyl-2-(4,5-diphenyl-1H-imidazol-2-yl)phenol (*p*-*t*Bu~dp): A mixture of 5-tert-butyl-2-hydroxybenzaldehyde (0.88 g, 4.95 mmol), benzil (1.04 g, 4.95 mmol) and ammonium acetate (7.00 g, 90.81 mmol) were reacted as for the preparation of ***o*-*t*Bu~dp**, but recrystallization was carried out in ethyl acetate to afford ***p*-*t*Bu~dp** (1.26 g, 69 %). Mp. 121-122 ^{o}C. Selected IR peaks (KBr, cm^{-1}): ν 3336m, 3280m, 3064m, 2968s, 1750s (acetic acid), 1718s (acetic acid), 1699s (acetic acid), 1645s, 1601m, 1396vs. ^{1}H NMR (400 MHz, TMS, $CDCl_3$); δ_{ppm} 9.65 (s, 2H); 7.57 (d, *J* = 6.8 Hz, 4H); 7.46 (s, 1H, phenol ring); 7.40-7.30 (m, 7H); 7.02 (d, *J* = 8.4 Hz, 1H, phenol ring); 1.34 (s, 9H, *t*-Bu); 2.23 (acetic acid adduct). ^{13}C NMR (100 MHz, $CDCl_3$): 176.80 (acetic acid), 155.21, 146.08, 141.63, 131.96, 119.61, 117.29, 111.63, 31.53, 20.72 (acetic acid), 18.33 (acetic acid). MS (EI) m/z 368 (M^+, 100 %): 368, 353, 325, 194, 165 Anal. Calc. for $C_{25}H_{24}N_2O{\cdot}1.5CH_3COOH$: C, 73.34; H, 6.59; N, 6.11 %. Found: C, 73.04; H, 6.90; N, 6.29 % (see Supplementary Information **S1**[46]).

4-(4,5-Diphenyl-1H-imidazol-2-yl)benzene-1,3-diol (*m*-H~dp): A mixture of 2,4-dihydroxybenzaldehyde (1.31 g, 9.51 mmol), benzil (2.00 g, 9.51 mmol) and ammonium acetate (14.00 g, 181.62 mmol) were reacted as for the preparation of ***o*-*t*Bu~dp**, but purified using 1:4 ethyl acetate / n-hexane on silica gel column to afford ***m*-H~dp** (2.12 g, 84 %). Mp. 110-111 ^{o}C.

Selected IR peaks (KBr, cm^{-1}): ν 3271s(br), 3059s, 1703s (ethyl acetate), 1604vs, 764s. ^{1}H NMR (200 MHz, TMS, d_6-dmso); δ_{ppm} 12.88 (s, 1H); 12.72 (s, 1H); 9.73 (s, 1H, phenolic OH); 7.83 (d, *J* = 9 Hz, 1H); 7.40 (m, 10H, 4,5-diphenyl); 6.39 (d, *J* = 2.2 Hz, 1H, phenol ring); 6.35 (s, 1H, phenol ring); 1.91 (ethyl acetate). ^{13}C NMR (50 MHz, d_6-dmso): 159.33, 158.40, 133.81. 133.48, 130.46, 128.68, 128.61, 128.41, 128.03, 126.84, 1265.68, 126.26, 126.03, 106.96, 104.91, 102.91, 21.07 (ethyl acetate), 14.04 (ethyl acetate). MS (EI) m/z 328 (M^+, 100 %): 299, 271, 165. Anal. Calc. for $C_{21}H_{16}N_2O_2 \cdot {}^3/_4$ethyl acetate: C, 73.72; H, 5.50; N, 7.35 %. Found: C, 73.56; H, 5.33; N, 7.37 %.

2-(4,5-Diphenyl-1H-imidazol-2-yl)benzene-1,4-diol (*p*-H~dp): A mixture of 2,5-dihydroxybenzaldehyde (0.66 g, 4.46 mmol), benzil (1.00 g, 4.46 mmol) and ammonium acetate (7.00 g, 90.81 mmol) were reacted as for the preparation of ***o*-*t*Bu~dp**, but purified using 1:2 ethyl acetate / n-hexane on silica gel column to afford ***p*-H~dp** (1.80 g, 74 %). Mp. 222-223 ^{o}C. Selected IR peaks (KBr, cm^{-1}): ν 3303s, 3194s, 3062s, 1650m, 1603s, 1586m, 1223vs. ^{1}H NMR (400 MHz, TMS, d_6-dmso); δ_{ppm} 12.91 (s, 1H); 12.22 (s, 1H); 8.92 (s, 1H); 7.54-7.39 (m, 8H, 4,5-diphenyl); 7.34 (dd, *J* = 7.2 Hz, 2H); 7.26 (dd, *J* = 7.2 Hz, 1H); 6.78 (d, *J* = 8.4 Hz, 1H, phenol ring); 6.73 (dd, *J* = 2.8, 8.8 Hz, 1H, phenol ring); ethylacetate. ^{13}C NMR (100 MHz, d_6-dmso): 150.07, 149.96, 146.42, 134.76, 129.19, 128.96, 128.69, 127.31, 117.62, 111.41. MS (EI) m/z 328 (M^+, 100 %): 328, 299, 271, 165. Anal. Calc. for $C_{21}H_{16}N_2O_2 \cdot {}^1/_8$ethyl acetate: C, 76.09; H, 5.05; N, 8.25 %. Found: C, 76.04; H, 5.07; N, 8.12 %.

Preparation of 2-(1H-Imidazol-2-yl)phenolatopalladium(II) Complexes

Preparation of the palladium complexes was achieved according to a similar general procedure and the case for **Pd(*o*-*t*Bu~dm)$_2$** will be presented as typical example. $Pd(AcO)_2$ (44 mg, 0.18 mmol) and ***o*-*t*Bu~dm** (86 mg, 0.36 mmol) were weighed into a 10 mL round-bottomed flask. After addition of about 2 mL absolute ethanol, the mixture was stirred for 12 hours at room temperature. The resulting orange precipitate was filtered, washed with few millilitres of ethanol and dried overnight at 60 ^{o}C to obtain **Pd(*o*-*t*Bu~dm)$_2$**.

In some of the preparations, diethyl ether, ethyl acetate or acetone was used as solvent in consideration of ligand solubility. Poor solubility in deuterated solvents hindered NMR measurements for some of the complexes. Synthetic and analytical data for the complexes are presented as follows:

Bis-[2-tert-butyl-6-(4,5-dimethyl-1H-imidazol-2-yl)phenolato]palladium(II) – Pd(*o*-*t*Bu~dm)$_2$: (55 mg, 52 %). Mp./Dec. ≈ 290 ºC. Selected IR peaks (KBr, cm^{-1}): ν 3412m, 2951s, 1628s, 1472vs, 753s. ^{1}H NMR (400 MHz, *d6*-dmso) δ 11.13 (s, 1H), 7.07 (d, *J* = 7.7 Hz, 1H), 6.93 (d, *J* = 7.6 Hz, 1H), 6.37 (t, *J* = 7.6 Hz, 1H), 2.53 (s, 3H), 2.21 (s, 3H), 1.19 (s, 9H). Anal. Calc. for $C_{30}H_{38}N_4O_2Pd{\cdot}EtAcO{\cdot}½H_2O$: C, 59.17; H, 6.86; N, 8.12 %. Found: C, 59.50; H, 6.27; N, 8.30 % (see Supplementary Information **S2**)[49].

Bis-[4-tert-butyl-2-(4,5-dimethyl-1H-imidazol-2-yl)phenolato]palladium(II) – Pd(*p*-*t*Bu~dm)$_2$: $Pd(AcO)_2$ (55 mg, 0.25 mmol) and ***p*-*t*Bu~dm** (120 mg, 0.50 mmol) gave **Pd(*p*-*t*Bu~dm)$_2$** as orange powder (138 mg, 93 %). Mp./Dec. > 300 ºC. Selected IR peaks (KBr, cm^{-1}): ν 3120m, 2962s, 1628s, 1495vs, 1254vs, 1054m. ^{1}H-NMR (400 MHz, *d6*-dmso): δ 12.32 (s, 1H), 7.76 (d, *J* = 2.3 Hz, 1H), 7.16 (dd, *J* = 8.6, 2.3 Hz, 1H), 6.78 (d, *J* = 8.6 Hz, 1H), 2.07 (s, 3H),

1.28 (s, 9H), 1.24 (s, 3H). Anal. Calc. for $C_{30}H_{38}N_4O_2Pd{\cdot}C_2H_5OC_2H_5$: C, 61.21; H, 7.25; N, 8.40 %. Found: C, 61.12; H, 7.42; N, 8.60 %.

Bis-[2-methoxy-6-(4,5-dimethyl-1H-imidazol-2-yl)phenolato]palladium(II) – Pd(*o*-M~dm)$_2$: $Pd(AcO)_2$ (23 mg, 0.10 mmol) and ***o*-M~dm** (45 mg, 0.21 mmol) gave **Pd(*o*-M~dm)$_2$** as orange powder (47 mg, 84 %). Mp./Dec. ≈ 292 ºC. Selected IR peaks (KBr, cm^{-1}): ν 3412m, 2950s, 1627s, 1592m, 1471vs, 1243vs, 753s. ^{1}H-NMR (400 MHz, *d6*-dmso): δ 12.23, 7.03 (dd, *J* = 8.0, 1.2 Hz), 6.60 (d, *J* = 6.7 Hz), 6.43 (t, *J* = 7.8 Hz), 3.56, 2.40, 2.17. Anal. Calc. for $C_{24}H_{26}N_4O_4Pd{\cdot}^1/_3EtOH{\cdot}^2/_3H_2O$: Elemental Analysis: C, 52.13; H, 5.20; N, 9.86 %. Found: C, 52.13; H, 5.21; N, 9.89 %.

Bis-[4-methoxy-2-(4,5-dimethyl-1H-imidazol-2-yl)phenolato]palladium(II) – Pd(*p*-M~dm)$_2$: $Pd(AcO)_2$ (51 mg, 0.23 mmol) and ***p*-M~dm** (109 mg, 0.46 mmol) gave **Pd(*p*-M~dm)$_2$** as orange powder (103 mg, 88 %). Mp./Dec. ≈ 290 ºC. Selected IR peaks (KBr, cm^{-1}): ν 3177m, 3125s, 3049s 2931ms, 1625m, 1608m, 1490vs, 1220vs, 1043s. ^{1}H-NMR (400 MHz, *d6*-dmso): δ 12.31 (s, 1H), 7.03 (d, *J* = 3.0 Hz, 1H), 6.61 (dd, *J* = 9.0, 3.0 Hz, 1H), 6.54 (d, *J* = 8.9 Hz, 1H), 3.68 (s, 3H), 2.28 (s, 3H), 2.18 (s, 3H). Anal. Calc. for $C_{24}H_{26}N_4O_4Pd$: C, 53.29; H, 4.84; N, 10.36 %. Found: C, 53.40; H, 4.43; N, 10.12 %.

Bis-[4-bromo-2-(4,5-dimethyl-1H-imidazol-2-yl)phenolato]palladium(II) – Pd(*p*-Br~dm)$_2$: $Pd(AcO)_2$ (56 mg, 0.25 mmol) and ***p*-Br~dm** (134 mg, 0.50 mmol) gave **Pd(*p*-Br~dm)$_2$** as orange powder (137 mg, 86 %). Mp./Dec. > 300 ºC. Selected IR peaks (KBr, cm^{-1}): ν 3192s, 3138s, 3050m 2977ms, 1624s, 1588m, 1474vs, 1279vs, 1144m. ^{1}H-NMR (400 MHz,

d6-dmso): δ 12.55, 7.64 (d, *J* = 2.6 Hz), 7.06 (dd, *J* = 8.8, 2.5 Hz), 6.58 (d, *J* = 8.9 Hz), 2.26, 2.17. Anal. Calc. for $C_{22}H_{20}Br_2N_4O_2Pd$: C, 41.37; H, 3.16; N, 8.77 %. Found: C, 41.55; H, 2.94; N, 8.84 %.

Bis-[2-tert-butyl-6-(4,5-diphenyl-1H-imidazol-2-yl)phenolato]palladium(II) – Pd(*o*-*t*Bu~dp)$_2$: $Pd(AcO)_2$ (69 mg, 0.31 mmol) and ***o*-*t*Bu~dp** (225 mg, 0.61 mmol) gave **Pd(*o*-*t*Bu~dp)$_2$** as orange powder (130 mg, 50 %). Mp./Dec. 231 ºC. Selected IR peaks (KBr, cm^{-1}): ν 3411s, 3179s, 3057s, 2951vs, 2911vs, 1705vs, 1597vs, 1441vs, 766vs. ^{1}H-NMR (400 MHz, *d6*-dmso): δ 12.91 (s, 1H), 8.58 (d, *J* = 7.5 Hz, 2H), 7.54 (t, *J* = 7.7 Hz, 2H), 7.38 (m, 7H), 6.84 (d, *J* = 6.4 Hz, 1H), 6.40 (t, *J* = 7.6 Hz, 1H), 0.74 (s, 9H). Anal. Calc. for $C_{50}H_{46}N_4O_2Pd{\cdot}EtOH$: C, 70.38; H, 5.91; N, 6.31 %. Found: C, 70.71; H, 5.59; N, 5.84 % (see Supplementary Information **S3**).

Bis-[4-tert-butyl-2-(4,5-diphenyl-1H-imidazol-2-yl)phenolato]palladium(II) – Pd(*p*-*t*Bu~dp)$_2$: $Pd(AcO)_2$ (82 mg, 0.37 mmol) and ***p*-*t*Bu~dp** (270 mg, 0.73 mmol) gave **Pd(*p*-*t*Bu~dp)$_2$** as orange powder (156 mg, 50 %). Mp./Dec. > 300 ºC. Selected IR peaks (KBr, cm^{-1}): ν 3611m, 3057s, 2954vs, 1612s, 1588m, 1489vs, 1251vs. Anal. Calc. for $C_{50}H_{46}N_4O_2Pd{\cdot}2H_2O$: C, 68.45; H, 5.74; N, 6.39 %. Found: C, 68.54; H, 5.82; N, 6.04 %.

Bis-[1-(4,5-diphenyl-1H-imidazol-2-yl)naphthalen-2-olato]palladium(II) – Pd(Naph~dp)$_2$: $Pd(AcO)_2$ (31 mg, 0.14 mmol) and **Naph~dp** (102 mg, 0.28 mmol) gave **Pd(Naph~dp)$_2$** (100 mg, 87 %). Single crystals of **Pd(Naph~dp)$_2$**·4thf) suitable for X-ray analysis was obtained by slow evaporation of solvent from it tetrahydrofuran (thf) solution.

Mp./Dec. > 300 ºC. Selected IR peaks (KBr, cm^{-1}): ν 3447s, 3185w, 3056s, 1612s, 1549s, 1371vs, 766vs. Anal. Calc. for $C_{50}H_{34}N_4O_2Pd \cdot 2EtOH$: C, 70.39; H, 5.03; N, 6.08. Found: C, 70.11; H, 4.91; N, 5.89.

Bis-[2-(4,5-diphenyl-1H-imidazol-2-yl)phenolato]palladium(II) – Pd(dp)$_2$: $Pd(AcO)_2$ (52 mg, 0.23 mmol) and **dp** (144 mg, 0.46 mmol) gave **Pd(dp)$_2$** as orange powder (87 mg, 51 %). Mp./Dec. 231 ºC. Selected IR peaks (KBr, cm^{-1}): ν 3162s, 3057s, 2965s, 1603s, 1557s, 1474vs, 1142m. Anal. Calc. for $C_{42}H_{30}N_4O_2Pd \cdot 1½EtOH \cdot H_2O$: C, 66.22; H, 5.06; N, 6.86 %. ^{1}H-NMR (400 MHz, *d6*-dmso): δ 11.65 (s, 1H), 7.93 (d, *J* = 8.2 Hz, 2H), 7.31 (m, 9H), 6.64 (m, 1H), 6.27 (m, 1H), 5.86 (d, *J* = 8.6 Hz, 1H). Found: C, 66.19; H, 4.86; N, 6.64 %. TG analysis: 151 – 180 ^{o}C, –10.30 % (tightly held solvent or water); 315 – 419 ^{o}C, –76 % (ligands).

Bis-[3-(4,5-diphenyl-1H-imidazol-2-yl)benzene-1,2-diolato]palladium(II) – Pd(*o*-H~dp)$_2$: $Pd(AcO)_2$ (43 mg, 0.19 mmol) and ***o*-H~dp** (126 mg, 0.35 mmol) gave **Pd(*o*-H~dp)$_2$** as orange powder (80 mg, 55 %). Mp./Dec. > 300 ºC. Selected IR peaks (KBr, cm^{-1}): ν 3398s, 3055m, 1617m, 1587m, 1479vs, 1241vs. ^{1}H-NMR (200 MHz, *d6*-dmso): δ 11.90 (s, 1H), 10.84 (s, 1H), 8.20 (d, *J* = 7.0 Hz, 2H), 7.35 (m, 8H), 6.30 (m, 2H), 5.22 (s, 1H). Anal. Calc. for $C_{42}H_{30}N_4O_4Pd \cdot 2H_2O$: C, 64.75; H, 4.96; N, 6.57 %. Found: C, 64.91; H, 4.92; N, 7.05 %.

Bis-[4-(4,5-diphenyl-1H-imidazol-2-yl)benzene-1,3-diolato]palladium(II) – Pd(*m*-H~dp)$_2$: $Pd(AcO)_2$ (63 mg, 0.28 mmol) and ***m*-H~dp** (186 mg, 0.57 mmol) gave **Pd(*m*-H~dp)$_2$** as orange powder (165 mg, 77 %). Mp./Dec. > 300 ºC. Selected IR peaks (KBr, cm^{-1}): ν 3528vs(sh), 3167s, 2964s, 1618vs, 1558vs, 1464vs, 1149vs. ^{1}H-NMR (400 MHz, *d6*-dmso): δ

12.59 (s, 1H), 8.97 (s, 1H), 7.81 (d, *J* = 7.4 Hz, 2H), 7.43 – 7.22 (m, 9H), 5.87 (dd, *J* = 8.6, 2.4 Hz, 1H), 5.29 (d, *J* = 2.3 Hz, 1H).Anal. Calc. for $C_{42}H_{30}N_4O_4Pd{\cdot}EtOH$: C, 65.47; H, 4.50; N, 6.94 %. Found: C, 65.37; H, 4.71; N, 6.51 %.

Bis-[2-(4,5-diphenyl-1H-imidazol-2-yl)benzene-1,4-diolato]palladium(II) – Pd(*p*-H~dp)$_2$: $Pd(AcO)_2$ (41 mg, 0.18 mmol) and ***p*-H~dp** (120 mg, 0.36 mmol) gave **Pd(*p*-H~dp)$_2$** as orange powder (111 mg, 80 %). Single crystals of **Pd(*p*-H~dp)$_2$**·4dmf suitable for X-ray analysis was obtained overnight by slow evaporation of solvent from it dmf solution. Mp./Dec. > 300 ºC. Selected IR peaks (KBr, cm^{-1}): ν 3254s, 3058s, 3026m, 1603w, 1587m, 1486vs, 1209vs, 1012m. ^{1}H-NMR (400 MHz, *d6*-dmso): δ 12.83 (s, 1H), 8.29 (s, 1H), 7.78 (d, *J* = 7.3 Hz, 2H), 7.41 – 7.20 (m, 8H), 6.99 (d, *J* = 2.9 Hz, 1H), 6.28 (dd, *J* = 8.8, 2.9 Hz, 1H), 5.63 (d, *J* = 8.8 Hz, 1H). Anal. Calc. for $C_{42}H_{30}N_4O_4Pd{\cdot}½H_2O$: C, 65.50; H, 4.06; N, 7.27. Found: C, 65.80; H, 3.85; N, 7.21. TG analysis: 99 – 273 ^{o}C, –2.26 % (tightly held water); 310 – 386 ^{o}C, –84 % (ligands).

Bis-[2-methoxy-6-(4,5-diphenyl-1H-imidazol-2-yl)phenolato]palladium(II) – Pd(*o*-M~dp)$_2$: $Pd(AcO)_2$ (112 mg, 0.50 mmol) and ***o*-M~dp** (340 mg, 0.99 mmol) reacted in acetone to give **Pd(*o*-M~dp)$_2$** as off-white micro-crystals (318 mg, 81 %). Mp./Dec. ≈ 260 ºC. Selected IR peaks (KBr, cm^{-1}): ν 3423vs, 3055m, 2967m, 1604vs, 1557m, 1540m, 1477vs, 1159, 764vs. ^{1}H-NMR (400 MHz, *d6*-dmso): δ 11.65 (s, 1H), 8.28 (d, *J* = 7.8 Hz, 2H), 7.37 – 7.29 (m, 8H), 6.98 (d, *J* = 7.8 Hz, 1H), 6.40 (d, *J* = 7.4 Hz, 1H), 6.24 (t, *J* = 7.7 Hz, 1H), 3.21 (s, 3H). Anal. Calc. for $C_{44}H_{34}N_4O_4Pd{\cdot}2H_2O{\cdot}CH_3COCH_3$: C, 63.91; H, 5.02; N, 6.34. Found: C, 64.25; H, 5.01; N, 6.23.

Bis-[2-(4,5-diphenyl-1H-imidazol-2-yl)-5-methoxyphenolato]palladium(II) – Pd(*m*-M~dp)$_2$: $Pd(AcO)_2$ (33 mg, 0.15 mmol) and ***m*-M~dp** (100 mg, 0.30 mmol) gave **Pd(*m*-M~dp)$_2$** as orange powder (100 mg, 87 %). Mp./Dec. > 300 ºC. Selected IR peaks (KBr, cm^{-1}): ν 3411vs, 3223s(br), 3057s, 2838s, 1656s, 1606vs, 1557m, 1488vs, 1155vs, 769vs. ^{1}H NMR (400 MHz, *d6*-dmso): δ 12.69 (s, 1H), 7.74 (d, *J* = 7.3 Hz, 2H), 7.52 (d, *J* = 8.8 Hz, 1H), 7.40 – 7.19 (m, 8H), 6.00 (dd, *J* = 8.7, 2.5 Hz, 1H), 5.22 (d, *J* = 2.5 Hz, 1H), 3.50 (s, 3H). Anal. Calc. for $C_{44}H_{34}N_4O_4Pd{\cdot}EtOH{\cdot}H_2O$: C, 64.75; H, 4.96; N, 6.57 %. Found: C, 64.34; H, 4.86; N, 6.71 %. TG analysis: 115 – 153 ^{o}C, –10.02 % (tightly held solvent or water); 307 – 397 ^{o}C, –78 % (ligands).

Bis-[2-(4,5-diphenyl-1H-imidazol-2-yl)-4-methoxyphenolato]palladium(II) – Pd(*p*-M~dp)$_2$: $Pd(AcO)_2$ (30 mg, 0.13 mmol) and ***p*-M~dp** (99 mg, 0.26 mmol) gave **Pd(*p*-M~dp)$_2$** as orange powder (92 mg, 89 %). Mp./Dec. ≈ 280 ºC. Selected IR peaks (KBr, cm^{-1}): ν 3423vs, 3055s, 2968m, 2830m, 1603s, 1588s, 1488vs, 1217vs, 766vs. ^{1}H NMR (400 MHz, *d6*-dmso): δ 12.87 (s, 1H), 7.77 (d, *J* = 7.4 Hz, 2H), 7.41 – 7.27 (m, 8H), 7.14 (d, *J* = 3.0 Hz, 1H), 6.38 (dd, *J* = 9.0, 2.9 Hz, 1H), 5.62 (d, *J* = 9.0 Hz, 1H), 3.62 (s, 3H). Anal. Calc. for $C_{44}H_{34}N_4O_4Pd{\cdot}EtOH{\cdot}½H_2O$: C, 65.44; H, 4.89; N, 6.64 %. Found: C, 65.22; H, 4.85; N, 6.35 %. TG analysis: 116 – 156 ^{o}C, –9.76 % (tightly held solvent species); 355 – 453 ^{o}C, –77 % (ligands).

Bis-[4-bromo-2-(4,5-diphenyl-1H-imidazol-2-yl)phenolato]palladium(II) – Pd(*p*-Br~dp)$_2$: $Pd(AcO)_2$ (71 mg, 0.31 mmol) and ***p*-Br~dp** (248 mg, 0.63 mmol) reacted in acetone to give **Pd(*p*-Br~dp)$_2$** as off-white micro-crystals (257 mg, 93 %). Mp./Dec. ≈ 285 ºC. Selected

IR peaks (KBr, cm^{-1}): ν 3173s, 3049s, 2965s, 2855s, 1600s, 1537s, 1474vs, 1290vs, 1051s. ^1H NMR (400 MHz, *d6*-dmso): δ 12.60 (s, 1H), 8.97 (s, 1H), 7.81 (d, *J* = 7.3 Hz, 2H), 7.46 – 7.23 (m, 8H), 5.88 (dd, *J* = 8.6, 2.4 Hz, 1H), 5.30 (d, *J* = 2.4 Hz, 1H). Anal. Calc. for $C_{42}H_{28}Br_2N_4O_2Pd{\cdot}EtOH$: C, 56.64; H, 3.67; N, 6.01 %. Found: C, 56.70; H, 3.65; N, 5.68 %.

Bis-[2-(4,5-diphenyl-1H-imidazol-2-yl)-4-nitrophenolato]palladium(II) – Pd(*p*-N~dp)$_2$: $Pd(AcO)_2$ (63 mg, 0.28 mmol) and ***p*-N~dp** (200 mg, 0.56 mmol) gave **Pd(*p*-N~dp)$_2$** (210 mg, 92 %). Mp./Dec. > 300 ºC. Selected IR peaks (KBr, cm^{-1}): ν 3400s, 3057s, 1605s, 1563m, 1303vs, 698s. Anal. Calc. for $C_{42}H_{28}N_6O_6Pd$: C, 61.58; H, 3.45; N, 10.26. Found: C, 61.69; H, 3.34; N, 10.24.

Bis-[5-methoxy-2-(1H-phenanthro[9,10-d]imidazol-2-yl)phenolato]palladium(II) – Pd(*m*-M~pt)$_2$: $Pd(AcO)_2$ (42 mg, 0.18 mmol) and ***m*-M~pt** (126 mg, 0.37 mmol) gave **Pd(m-M~pt)$_2$** after the product, which is very soluble in ethanol, was precipitated by addition of hexane (75 mg, 52 %). Mp./Dec. ≈ 270 ºC. Selected IR peaks (KBr, cm^{-1}): ν 3434s, 3307s, 3062s, 2965m, 1634vs, 1606vs, 1524vs, 754vs. Anal. Calc. for $C_{44}H_{30}N_4O_4Pd.{}^2/_3C_6H_{14}$: C, 68.42; H, 4.71; N, 6.65 %. Found: C, 68.88; H, 4.31; N, 6.59 %.

Bis-[4-methyl-2,6-bis(4,5-diphenyl-1H-imidazol-2-yl)phenolato]palladium(II) – Pd(Bis-Im)$_2$: $Pd(AcO)_2$ (56 mg, 0.25 mmol) and **Bis-Im** (273 mg, 0.50 mmol) gave **Pd(Bis-Im)$_2$** (219 mg, 75 %). Mp./Dec. > 300 ºC. Selected IR peaks (KBr, cm^{-1}): ν 3403vs, 3055s, 2919w, 1604s, 1481vs, 696vs. Anal. Calc. for $C_{74}H_{54}N_8O_2Pd$: C, 74.46; H, 4.56; N, 9.39 %. Found: C, 74.88; H, 4.47; N, 9.30 %.

Suzuki-Miyaura Cross-Coupling Experiments

In typical reactions, (4-Bromophenyl)methanol (187 mg, 1.0 mmol) was reacted with either 4-acetylphenylboronic acid (197 mg, 1.2 mmol), 3,5-dimethylphenylboronic acid (180 mg, 1.2 mmol) or 2-bromophenylboronic acid (240 mg, 1.2 mmol) in the presence of a given palladium(II) complex (0.2 mol %) as catalyst precursor, K_2CO_3 (207 mg, 1.5 mmol) as base and 3 mL dmf / 1 mL H_2O mixture as solvent. Yields were calculated by carrying out ^{1}H-NMR analyses on the reaction mixtures through comparison of peak integration values for the methanolyl –CH_2– signal on (4-bromophenyl)methanol (the aryl-bromide substrate, $\delta \approx 4.5$ ppm) with that of the biphenyl products ($\delta \approx 4.7$ ppm). Catalysis reaction products [1-(4'-(hydroxymethyl)biphenyl-4-yl)ethanone (**1**) and (3',5'-dimethylbiphenyl-4-yl)methanol (**2**)] were purified by column chromatography on silica gel and characterized. In the case of 2-bromo-4'-methanolylbiphenyl (**3**), catalysis only gave trace yield as monitored by TLC and ^{1}H-NMR. Analytical data of the coupled products are as follows:

1-(4'-(hydroxymethyl)biphenyl-4-yl)ethanone (1): ^{1}H NMR (400 MHz, TMS, $CDCl_3$); δ_{ppm} 8.01 (d, *J* = 8.0 Hz, 2H); 7.66 (d, *J* = 8.4 Hz, 2H); 7.61 (d, *J* = 8.4 Hz, 2H); 7.45 (d, *J* = 8.0 Hz, 2H); 4.75 (s, 2H, –CH_2–); 2.62 (s, 3H, acetyl). ^{13}C NMR (400 MHz, $CDCl_3$): 197.71 (carbonyl), 141.00, 139.23, 135.92, 128.93, 127.53, 127.45, 127.15, 64.96 (methanolyl), 26.63 (methyl). MS (EI) m/z 226 (M^+, 98 %): 226, 211, 165, 152. Anal. Calc. for $C_{15}H_{14}O_2$: C, 79.62; H, 6.24 %. Found: C, 79.52; H, 6.31 %.

(3',5'-dimethylbiphenyl-4-yl)methanol (2): ^{1}H NMR (400 MHz, TMS, $CDCl_3$); δ_{ppm} 7.58 (d, *J* = 8.0 Hz, 2H, *p*-substituted phenyl); 7.42 (d, *J* = 8.0 Hz, 2H, *p*-substituted phenyl); 7.22 (s, 2H, dimethyl-substituted phenyl); 7.01 (s, 1H, dimethyl-substituted phenyl); 4.74 (s, 2H, methylene); 2.39 (s, 6H, dimethyl). ^{13}C NMR (400 MHz, $CDCl_3$): 140.91, 140.84, 139.69, 138.30, 131.64, 128.98, 128.58, 127.35, 125.03, 65.18 (methanolyl), 21.40 (dimethyl).

Results and discussion

Syntheses and Characterization of 2-(1H-imidazol-2-yl)phenols and their Palladium(II) Complexes

The electronically and structurally varied 2-(1H-imidazol-2-yl)phenol ligands were prepared using rationally selected salicylaldehydes and α-dicarbonyls, which were condensed in the presence of ammonium acetate while acetic acid played the dual role of solvent and catalyst for the condensation.[50] The palladium(II) complexes were generally obtained in good yields by room temperature reaction between $Pd(AcO)_2$ and individual members of the ligand series in suitable solvent media. Elemental analyses and spectroscopic data gave agreement with the identity of ligands and palladium complexes. Characterization analyses frequently revealed presence of solvent adducts in the synthesized azole compounds and the occurrence of hydrogen-bonded polar solvents like ethanol, ethylacetate, water, dimethylformamide, etc., has been evidenced by single crystal and NMR analyses.[39-45,46,47] There is high propensity for 1H-imidazole moieties to strongly hold nearby polar functions via intermolecular or intramolecular hydrogen-bonding. Furthermore, according to CHN analyses and ^{1}H NMR results, the solvent adducts are often present in non-stoichiometric amounts after samples have been air- or oven-dried. However, the analyses for crystallized samples submitted without prolonged air-drying

attempts usually showed stoichiometric presence of the adduct solvents in accordance with crystal structure composition of complex-to-solvent ratios.[40,41,44,45] Thermogravimetric analysis (TGA) data obtained for the complexes frequently revealed initial weight loss values ranging from 1 % to 14 % at about 100 – 200 ^{o}C, which could be attributed to loss of some tightly held solvents (see Supplementary Information **S4**).[46]

X-ray Structural Characterization Results

Crystal structures solved for complexes **Pd(de)$_2$**, **Pd(*o*-*t*Bu~dp)$_2$**, **Pd(Naph~dp)$_2$** and **Pd(*m*-M~pt)$_2$** are presented as representative structural characterization data for the target palladium complex series according to **Scheme 1** (**Fig. 1 – 4**, **Table 1**). Suitable single crystals for complexes **Pd(de)$_2$**, **Pd(Naph~dp)$_2$** and **Pd(*m*-M~pt**) grow by slow evaporation from solution of the synthesized complexes in dimethylformamide, tetrahydrofuran and ethanol respectively. On the other hand, red single crystal blocks of **Pd(*o*-*t*Bu~dp)$_2$** grow when palladium acetate and ***o*-*t*Bu~dp** are allowed to stand overnight in diethyl ether.

Pd(de)$_2$, **Pd(Naph~dp)$_2$** and **Pd(*m*-M~pt)$_2$** crystallize in the monoclinic (P2(1)/c or P2(1)/n) space group while **Pd(*o*-*t*Bu~dp)$_2$** crystallizes in the triclinic P-1 space group. Their experimental processing parameters are presented in **Table 1** below. The observed diversity in the pattern of solvent bonding to the imidazole functions is noteworthy because it suggests presence of strong solute-solute interaction capabilities at the 1H-imidazole moieties of these compounds. It also serves as evidence for the observed solvent adducts found in NMR, CHN and TGA. During experiment for slow solvent evaporation from dmf solution of **Pd(de)$_2$** according to our recently reported synthesis,[48] two crystal habits were observed; the compound crystallizes as red-orange hexagonal crystal discs containing discrete dmf adducts of **Pd(de)$_2$***2dmf (**Fig. 1**)

and light-green needles containing **Pd(de)$_2$***dmf*H_2O[48] in which dmf and water molecules aided formation of hydrogen-bonded, 1-dimensional networks. The complexe **Pd(Naph~dp)$_2$** (**Fig. 2**) also crystallizes as discrete, hydrogen-bonded thf adduct units. However, the structural result for **Pd(*m*-M~pt)$_2$** revealed a 2-dimentional hydrogen bonding network mediated by EtOH molecules. The inclusion of dmf, thf, water, diethyl ether or ethanol solvent molecules by varying modes of solvent-solute interactions in the analyzed structures is consistent with observations in the analytical characterization data.

Structural Evidence of Cyclometallation Tendencies Obtained from Species In Filtrates of Some Complexation Reactions

Owing to the N^O heteroatoms, ligand frameworks prepared towards this study were expected to coordinate as bidentate mono-anionic chelators in the ratio of two ligand molecules to one palladium(II) ion in order to yield neutral bis-ligated complexes. As presented above, analytical data for precipitate of complexation reactions show agreement with the bis-ligated coordination. However, some unexpected organometallic coordination species believed to be in small amounts were encountered / isolated from some filtrates (mother liquors). As much as possible and as a routine in the course of syntheses of complexes in this work, individual reaction filtrates were collected in clean tubes or vials and allowed to undergo slow evaporation in attempts to possibly grow single crystals of the target bis-ligated complexes. While only crystals of anticipated palladium complexes grew from some of the complexation filtrate solutions (**Fig. 4** and Supplementary Information **S5**), some members of the 2-(4,5-diphenyl-1H-imidazol-2-yl)phenol ligand series (**Scheme 1(b)**) produced mainly microcystals / powders of target complexes along with few (1-5) blocks of crystals, which were found to contain tridentate C^N^O cyclometallation species in which the palladium metal centre is coordinated to an *ortho*-

carbon position on the nearby phenyl (**Scheme 2(a)**). Thus, the second set of structural results shown in **Figures 5 – 7** presents the evidence for the tendency to form of cyclometallated species by certain ligand frameworks and this may suggest chelate stability as well as consequent tendency for catalyst inactivity for complexes bearing such ligands. It may be reasonable to conclude that higher chelate stability from cyclometallating ligands would reduce the number of coordination sites around the active metal centre especially with palladium(II) that is restricted to coordination number 4.

Specifically, ^{cy}**Pd(*p*-Br~dp)$_2$**, ^{cy}**Pd$_3$(*o*-M~dp.AcO)$_2$** and ^{cy}**Pd$_4$(*p*-N~dp)$_4$** crystallized alongside precipitation of the target complexes **Pd(*p*-Br~dp)$_2$**, **Pd(*o*-M~dp)$_2$** and **Pd(*p*-N~dp)$_2$** and the structure refinement data for the cyclometallated species are collected in **Table 2**. It is noteworthy that the single crystal sample of ^{cy}**Pd(*p*-Br~dp)$_2$** grew as a single colourless block. It could be reasoned that the influence of electron-withdrawing functions (i.e. *p*-bromo-, *o*-methoxy- or *p*-nitro-substituents) on the phenolate oxygen-donor limits the donor strength of the anionic oxygen-donor atom and the consequently higher electrophilicity of the palladium(II) center probably favours the formation of tridentate cyclometallation species. The concept of *ortho,para*-direction may also need to be considered in respect of the relative position of the *p*-bromo-, *o*-methoxy- or *p*-nitro-substituents to the carbon bearing the phenolate oxygen-donor. **Table 3** contains data for comparison of selected bond lengths and angles. The observed values are within usual range. The Pd1–O1 bond lengths are all longer for the cyclometallated complexes (**Figures 5 – 7**) than for the bis-ligated complexes (**Figures 1 – 4**) and the reverse is the case for the Pd1–N1. This may be considered to the conclusion of weaker metal to oxygen-

donor bonds on the ligand frameworks experiencing electron-withdrawing effects on the phenolate ring as described above. Furthermore, the torsion angles (C1-C6-C7-N1), which are smaller for the cyclometallated complexes, provides information on general co-planarity of the imidazole-phenol rings. The higher co-planarity of the imidazole-phenol rings in the tridentate organometallic species (**Figures 5 – 7**) suggests rigidity and coordination stability.

Study of Catalytic Efficiencies as Consequence of Cyclometallation, Steric and Electronic Properties

The series of palladium complexes were individually examined for their efficiencies as catalyst in Suzuki-Miyaura cross-coupling reactions in efforts to understand the influence of the systematically varied characteristics of coordinated organic frameworks towards obtaining superior palladium(II) active species. **Scheme 3** presents the coupling experiments carried out in this study. The reason for using (4-bromophenyl)methanol as the arylbromide substrate is because of utility of its methylene (–CH_2–) ^{1}H-NMR signals in the 4 – 5 ppm chemical shift region (**Fig. 8**). The absence of interfering NMR signals enables clear observation of the respective methylene peaks for the C-C coupled biphenyl products and that of the arylbromide reactant. **Fig. 8** shows NMR spectral stack for a reaction mixture before reflux, at intervals (30 min, 60 min, 120 min) and after purification of the coupling product. Therefore, reliable estimation of the relative amounts of reactants and products present in a given catalytic reaction mixture is achieved by comparison of peak integration values.

In the first instance, (4-acetylphenyl)boronic acid was coupled with (4-bromophenyl)methanol. As presented in **Table 4**, **Pd(de)$_2$** (0.2 mol %) was utilized under various conditions of temperature, reflux duration, presence of base additive and solvent media

in order to establish a suitable set of reaction parameters under which the catalytic behaviours of the series of complexes would be comparatively evaluated. Results showed that presence of water as well as base additive is important for the coupling reaction (**Table 4**; entries 2 and 4) and that acetone proved to be unfavourable solvent (**Table 4**; entry 3). Furthermore, temperatures below 100 ^{o}C were found to be unfavourable for the C – C coupling catalysis (**Table 4**; entry 5) and this suggests that the palladium pre-catalysts require some sort of thermal decomposition in order to make some coordination sites free around the metal centre. The 16.7 % yield for entry 6 of **Table 4** was considered to be appropriate because it would enable detection of higher catalyst activities when the various complexes are evaluated. It was therefore concluded that the conditions for further experiments for evaluation of catalytic behaviour of the series of palladium complexes would be 30 min reflux at 100 ^{o}C using 4 mL of 3:1 dmf/H_2O solvent mixture in the presence of potassium carbonate (1.5 mol equivalent relative to substrate) and 0.2 mol % of the individual palladium compounds.

Catalytic data for all the palladium pre-catalysts were collected under the chosen general condition (100 ^{o}C, 3:1 dmf/H_2O mixture, 1.5 mol. equivalent of potassium carbonate, 30 min reflux duration and 0.2 mol % palladium complex loading) and they are collected in **Table 5**. For comparison, the same coupling experiment was also conducted in the presence of palladium acetate alone as catalyst and a yield of 29 % was obtained (**Table 5**; Entry 1). Furthermore, in attempts to ascertain trends and preferences especially for complexes having higher catalyst activities, shorter reflux duration, other solvent media and adjusted temperatures were also studied. For ease of comparison, the yields and corresponding turnover frequencies for all the complexes have been presented in a bar chart (**Fig. 9 (a)** and **(b)**).

Consideration of catalyst activities for the first series of palladium complexes bearing the methyl- or ethyl-substituted imidazoles and for which ligand based steric bulk is absent, suggest that presence of sterically bulky organic frameworks around the active palladium centre is not necessarily a condition for high catalyst efficiency contrary to recent conclusions.[5,51] The complexes bearing electron-releasing-groups generally yielded lower turnover frequencies (TOFs) than obtained for the reaction catalyzed by the ligand-free palladium acetate (**Table 5**; Entry 1 vs Entries 2 – 4) and this is attributable to the stronger N^O bidentate chelation stability. Conversely, the palladium complexes bearing electron-withdrawing-groups (EWGs; bromo-, nitro-) on the phenolate ring yielded high catalyst efficiencies (**Table 5**; Entries 7 – 9; **Fig. 9 (a)** and **(b)**). It could be concluded that the poorer catalytic behaviour for complexes of **de**, ***o*-*t*Bu~dm**, ***p*-*t*Bu~dm**, ***o*-M~dm** and ***p*-M~dm** is attributable to stronger N^O chelation stabilities while higher catalyst activities, which is consequent on the presence of the electron-withdrawing-groups and resultant poorer donor character of the phenolate oxygen-donors of ligands ***p*-Br~dm** and ***p*-N~dm**, is attributable to poorer chelate stabilities. These results support the conclusion that hemilabile ligands on palladium complexes, which possess tendency for easy conversion from chelation to monodentate coordination mode under catalysis condition, would be beneficial to catalytic efficiency.[5,46,47] The monodentate coordination by one of the ***p*-Br~dp** ligands in **Fig. 5** lends support to the conclusion that electron withdrawing groups at the *para*-position tends to reduce the coordination character of the phenolate oxygen-donor atom and the same conclusion has been crystallographically evidenced by observed double bond character of a phenol C–O bond in the presence of *p*-nitro substituent.[46] **Pd(*p*-Br~dm)$_2$** showed the highest activity under the 30 min reflux duration (**Table 5**; Entry 7ii; TOF = 779 h^{-1}) and similar result was obtained when catalysis was carried out by *in situ* method of generating active species

(**Table 5**; Entry 8ii; TOF = 800 h^{-1}). However, comparison of catalytic outcome at 30 min reflux with outcomes under shorter reflux time of 15 min for **Pd(*p*-Br~dm)$_2$** as pre-catalyst or via '**Pd(AcO)$_2$** + ***p*-Br~dm**' *in situ* catalyst generation method revealed that initial rate is notably higher for the *in situ* catalyst formation method leading to higher TOF (**Table 5**; Entry 7i vs Entry 8i; **Fig. 9 (a)** and **(b)** and **Fig. 10**); i.e. the active species are probably formed faster via the *in situ* 'salt+ligand' catalyst generation method. In general, results for the methy / diethyl (**dm** / **de**) ligand frameworks suggest that electronic properties of the organic ligands possess very important influence on catalytic outcomes relative to steric characters.

On the other hand, the complex series ligated by the 4,5-diphenyl-1H-imidazole ligands only showed high catalyst activities for **Pd(*o*-*t*Bu~dp)$_2$** and **Pd(Naph~dp)$_2$**. Their ligands possess moieties that tend to sterically hamper the anticipated bidentate coordination; i.e. in addition to the steric demands resulting from the presence of pendant phenyl ring on the imidazole side of the N^O chelating atoms, there is further provision of steric hindrance towards coordination by *t*Bu group *ortho* to the coordinating phenolate oxygen-donor atom in **Pd(*o*-*t*Bu~dp)$_2$** (**Table 5**; Entry 10; TOF = 845 h^{-1}) and naphthol moiety, which suffers steric hindrance from the 1H-imidazole proton thereby widening the bite angle via loss of imidazole-naphthol co-planarity in **Pd(Naph~dp)$_2$** (**Table 5**; Entry 12ii; TOF = 872 h^{-1} at 30 min reflux) (**Scheme 2(b)**). The highly active **Pd(Naph~dp)$_2$** was also evaluated at 15 minutes and found to show high initial rate as presented in **Fig. 9 (a)** and **(b)** and **Fig. 10**. It is noteworthy that the crystal structural data revealed higher C1-C6-C7-N1 torsion angles (i.e. measure of loss of co-planarity between imidazole and phenol / naphthol rings; **Table 3**; 2nd and 3rd entry rows) for the catalytically efficient 4,5-diphenyl-1H-imidazole complexes (**Scheme 2(b)**). Therefore, their chelation stabilities for the N^O bidentate coordination mode would be weaker with consequent

ease of generating N-bonded monodentate coordination species at catalysis temperature. The structurally observed tendency for formation of palladacyclic species appeared to portend very unfavourable consequences for catalytic benefits of the complex derivatives bearing 4,5-diphenyl-1H-imidazole ligands.

It could be anticipated that, for **Pd(*p*-Br~dp)$_2$** (Entry 20; TOF = 46 h^{-1}; **Table 5**) and **Pd(*p*-N~dp)$_2$** (**Table 5**; Entry 21; TOF = 48 h^{-1}), the presence of nitro- and bromo-substitution at *para* position relative to the phenol hydroxyl position would induce similar high catalyst activities as a result of poor phenolate oxygen-donor characteristics as observed in the case of dimethylimidazole / diethylimidazole complexes. However, the opposite influence was obtained in which the ligands appeared to effectively poison the catalyst potential of the palladium metal centre. The lowest catalytic efficiencies (yield ≈ 5 %) observed for the bromo- and nitro-substituted 4,5-diphenyl-1H-imidazole complexes indicate absence of any useful amounts of active palladium metal centres in the catalysis experiments catalyzed by **Pd(*p*-Br~dp)$_2$** or **Pd(*p*-N~dp)$_2$** and, based on structural evidence, this outcome is compatible with the above thinking that formation of tridentate N^O^C palladacycle species via cyclometallation between the palladium metal and nearby phenyl ring is favoured by the presence of electron withdrawing groups on the phenol ring. Presence of cyclometallation tendency might be responsible for the generally poor catalyst efficiencies of the 4,5-diphenyl-1H-imidazole complex derivatives. The values of TOFs obtained for the *ortho*-, *meta*- and *para*-substituted analogues **Pd(*o*-H~dp)$_2$**, **Pd(*m*-H~dp)$_2$** and **Pd(*p*-H~dp)$_2$** (**Table 5**; Entries 14 – 16; TOF = 478, 167 and 84 h^{-1} respectively) apparently suggest that the electron-withdrawing character of the substituent hydroxyl group is strongest at the *para*-position and that the consequently higher cyclometallation tendency in **Pd(*p*-H~dp)$_2$** is responsible for its low catalyst relevance.

Furthermore, the wide difference in catalytic efficiency of the phenanthrenyl complex **Pd(*m*-M~pt)$_2$** (**Table 5**; Entry 22i; TOF = 940 h^{-1}; highest yield) and its analogous diphenyl complex **Pd(*m*-M~dp)$_2$** (**Table 5**; Entry 18; TOF = 142 h^{-1}) probably supports presence of N^O^C chelation effects in **Pd(*m*-M~dp)$_2$** despite the electron-rich character of their methoxy-substituent. The fused and rigid phenanthrenyl rings of **Pd(*m*-M~pt)$_2$** would prevent cyclometallation and contribute steric hindrance towards coordination, which may favour easy formation of N-coordinated monodentate species at catalysis temperature. In summary, results obtained in this work suggest that catalytic outcomes are mainly dependent on chelation modes (i.e. whether N, N^O or N^O^C is stable), which could be influenced by steric / electronic properties of substituent moieties born on the ligands. It was observed that the higher the tendency to form stable multidentate chelate coordination around a palladium metal centre the more catalytically inactive such palladium metal centre becomes. Moreover, the catalytically active complexes appear to possess ligands with poorer chelation properties, which would readily furnish monodentate coordination species at catalysis temperature and which are not necessarily sterically bulky. According to **Fig. 9 (a)**, the highest catalytic yields obtained from complex pre-catalysts in this work pertained to complexes **Pd(*p*-Br~dm)$_2$** (Table 5; Entry 7ii; 77.9 %), **Pd(Naph~dp)$_2$** (Table 5; Entry 12ii; 87.2 %) and **Pd(*m*-M~pt)$_2$** (Table 5; Entry 22i; 94.0 %). However, the TOF data (**Fig. 9 (b)**) indicated that **Pd(Naph~dp)$_2$** possessed superior catalyst capacity on the basis of reduced time (**Fig. 10**). Therefore, **Pd(Naph~dp)$_2$** was employed as pre-catalyst towards other arylboronic acids and results suggests that the pre-catalyst is favourable towards diverse electronically substituted arylboronic acid reagent, but not favourable towards sterically challenged substrates (**Table 6**).

Conclusion

Series of sterically and electronically varied 2-(1H-imidazol-2-yl)phenol ligand frameworks have been designed towards preparation of palladium complexes, which were properly characterized. Single crystal structures of products precipitated from complexation reactions proved that targeted bis-ligand Pd(N^O)$_2$ complexes were obtained. However, X-ray diffraction analyses of the few crystals obtained from slow evaporation of filtrate solutions recovered during isolation of complexation precipitates for reactions involving 2-(4,5-diphenyl-1H-imidazol-2-yl)phenol derivatives provided evidence for formation of little amounts of N^O^C chelate species, which remain in solution.

In summary, results obtained in this work suggest that catalytic outcomes are mainly dependent on which chelation mode is favoured, which could be influenced by steric / electronic properties of substituent moieties born on the ligands. It was observed that the higher the tendency to form stable multidentate chelate coordination around a palladium metal centre the more catalytically inefficient such palladium metal centre would be. Furthermore, the catalytically active complexes generally possess ligands with poorer chelation properties, which imply that they would easily form monodentate coordination species at catalysis temperature. Good catalyst behaviour of **Pd(*p*-N~dm)$_2$** and **Pd(*p*-Br~dm)$_2$** suggests that suitable ligands should not necessarily be sterically bulky. **Pd(Naph~dp)$_2$** was employed as pre-catalyst towards other arylboronic acids and results suggests that the pre-catalyst is favourable towards diverse electronically substituted arylboronic acid reagent, but not favourable towards sterically challenged substrates.

Structural and catalytic results in this work indicate that ligand hemilability and sterically hindered chelation character, which facilitate ease of forming monodentate imidazole N-coordinated species at the catalysis reflux temperature, are favourable for obtaining superior catalyst activities. It was also concluded that presence of potential for cyclometallation in a palladium complex will significantly frustrate catalyst activity of its metal centre.

Supplementary Information

CCDC 879232 – 879234, 962566, 962567, 965788 and 965789 contain the supplementary crystallographic data for this paper. These data can be obtained free of charge via *www.ccdc.cam.ac.uk/data_request/cif* from the Cambridge Crystallographic Data Centre.

Acknowledgement

A.O.E is grateful to the Redeemer's University Research Grants Committee for supports with laboratory facilities. The financial support by the Deutsche Forschungsgemeinschaft (DFG) is gratefully acknowledged (PL 155/11, PL 155/12 and PL155/13).

References

1. X. Wang, F.-D. Liu , H.-Y. Tu, A.-D. Zhang. *J. Org. Chem.*, 2014, **79**, 6554–6562.
2. K. A. Netland, A. Krivokapic, M. Schröder, K. Boldt, F. Lundvall, M. Tilset. *J. Organomet. Chem*., 2008, **693**, 3703–3710
3. P. Espinet, A. M. Echavarren. *Angew. Chem., Int. Ed*., 2004, **43**, 4704–4734.
4. H. Doucet, J.-C. Hierso. *Angew. Chem., Int. Ed*., 2007, **46**, 834–871.
5. T. E. Barder, S. L. Buchwald. *Org. Lett.*, 2004, **6**, 2649–2652.
6. S. T. Marshall, M. O'Brien, B. Oetter, A. Corpuz, R. M. Richards, D. K. Schwartz, J.W. Medlin. *Nature Materials*, 2010, **9**, 853–858.
7. T. Thaler, B. Haag, A. Gavryushin, K. Schober, E. Hartmann,R. M. Gschwind, H. Zipse, P. Mayer, Paul Knochel. *Nature Chem.*, 2010, **15**, 125–130.
8. P.-X. Zhou, Y.-Y. Ye, J.-W. Ma, L. Zheng, Q. Tang, Y.-F. Qiu, B. Song, Z.-H. Qiu, P.-F. Xu, Y.-M. Liang. *J. Org. Chem.*, 2014, **79**, 6627–6633.
9. J. G. de Vries. *Dalton Trans.*, 2006, **2006**, 421–429.
10. G. A. Molander, S. R. Wisniewski. *J. Org. Chem.*, 2014, **79**, 6663–6678.
11. K. Watanabe, T. Mino, T. Abe, T. Kogure, M. Sakamoto. *J. Org. Chem.*, 2014, 79 (14), pp 6695–6702.
12. A. Suzuki. *Tet. Lett*., 1981, **22**, 127–130.
13. N. Miyaura, K. Yamada, A. Suzuki. *Tet. Lett*., 1979, **20**, 3437–3440.
14. E. Negishi, H. Matsushita, N. Okukado. *Tet. Lett*., 1981, **22**, 2715–2713.
15. E. Negishi, H.-J. Matsushita, M. Kobayashl, C. L. Rand. *Tet. Lett*., 1983, **24**, 3823–3824.
16. E. Negishi, T. Takahashi, K. Akiyoshi. *J. Organomet. Chem*., 1987, **334**, 181–194.
17. H. A. Dieck, F. R. Heck. *J. Organomet. Chem*., 1975, **93**, 259–263.

18. M. Qian, E. Negishi. *Tet. Lett*., 2005, **46**, 2927–2930.

19. G. Shore, S. Morin, D. Mallik, M. G. Organ. *Chem. A Eur. J*., 2008, **14**, 1351–1356.

20. M. Miura. *Angew. Chem., Int. Ed*. 2004, **43**, 2201–2203.

21. R. Chinchilla, C. Najera. *Chem. Rev*., 2007, **107**, 874–922.

22. N. Miyaura, A. Suzuki. *Chem. Rev*., 1995, **95**, 2457–2483.

23. E. A. B. Kantchev, C. J. O'Brien, M. G. Organ. *Angew. Chem., Int. Ed*., 2007, **46**, 2768–2813.

24. E. Peris, R. H. Crabtree. *Coord. Chem. Rev*., 2004, **248**, 2239–2246.

25. A. F. Littke, G. C. Fu. *Angew. Chem., Int. Ed*., 2002, **41**, 4176–4211.

26. Z. Weng, S. Teo, T. S. A. Hor. *Acc. Chem. Res*., 2007, **40**, 676–684.

27. N. T. S. Phan, M. Van Der Sluys, C. W. Jones. *Adv. Synth. Catal*., 2006, **348**, 609–679.

28. J. A. Widegren, R. G. Finke. *J. Mol. Catal. A: Chem*., 2003, **198**, 317–341.

29. D. Astruc, *Inorg. Chem.*, 2007, **46**, 1884–1894.

30. D. N. Korolev, N. A. Bumagin. *Tet. Lett*. 2006, **47**, 4225–4229.

31. E. R. Strieter, D. G. Blackmond, S. L. Buchwald. *J. Am. Chem. Soc*., 2003, **125**, 13978–13980.

32. S. D. Walker, T. E. Barder, J. R. Martinelli, S. L. Buchwald. *Angew. Chem.*, 2004, **116**, 1907–1912.

33. W. Chen, C. Xi, Y. Wu. *J. Organomet. Chem*., 2007, **692**, 4381–4388.

34. J. Ruiz, C. Vicente, N. Cutillas, J. Pérez. *Dalton Trans*., 2005, **2005**, 1999–2006.

35. A. Kumar, M. Agarwal, A. K. Singh. *J. Organomet. Chem.* 2008, **693**, 3533–3545.

36. E. Tas, A. Kilic, M. Durgun, I. Yılmaz, I. Ozdemir, N. Gurbuz. *J. Organomet. Chem*., 2009, **694**, 446–454.

37. M. Cai, Q. Xu, Y. Huang. J. *Mol. Catal. A*., 2007, **271**, 93–97.

38. P. D. Stevens, G. Li, J. Fan, M. Yen, Y. Gao. *Chem. Commun*., 2005, **2005**, 4435–4437.

39. A. O. Eseola, W. Li, R. Gao, M. Zhang, X. Hao, T. Liang, N. O. Obi-Egbedi, W.–H. Sun. *Inorg. Chem*., 2009, **48**, 9133–9146.

40. A. O. Eseola, M. Zhang, J.-F. Xiang, W. Zuo, Y. Li, J. A. O. Woods, W.-H. Sun. *Inorg. Chim. Acta*, 2010, **363**, 1970–1978.

41. A. O. Eseola, W. Li, O. G. Adeyemi, N. O. Obi-Egbedi, J. A. O. Woods. *Polyhedron*, 2010, **29**, 1891–1901.

42. A. O. Eseola, N. O. Obi-Egbedi. *Spectrochim. Acta A. Mol. and Biomol. Spec.* 2010, **75**, 693–701.

43. A. O. Eseola, W.-H. Sun, W. Li, J. A. O. Woods. *J. Mol. Str*. 2010, **984**, 117–124.

44. A. O. Eseola, W. Li, W.-H. Sun, M. Zhang, L. Xiao, J. A. O. Woods. *Dyse & Pigments*, 2011, **88**, 262–273.

45. A. O. Eseola, O. Adepitan, H. Görls, W. Plass. *New J. Chem*., 2012, **36 (4)**, 891–902**.**

46. A. O. Eseola, O. Akogun, H. Görls, O. Atolani, G. A. Kolawole, W. Plass. *J. Mol. Catal. A.* 2014, **387,** 112–122.

47. A. O. Eseola, D. Geibig, H. Görls, W.-H. Sun, X. Hao, J. A. O. Woods, W. Plass. *J. Organomet. Chem.* 2014, **754**, 39–50.

48. G. M. Sheldrick. *Acta Cryst. A*, 2008, **A64**, 112–122.

49. G. R. Fulmer, A. J. M. Miller, N. H. Sherden, H. E. Gottlieb, A. Nudelman, B. M. Stoltz, J. E. Bercaw, K. I. Goldberg. *Organometallics*, 2010, **29**, 2176–2179.

50. M. Yamada, Y. Tanaka, Y. Yoshimoo, S. Kuroda, I. Shimao. *Bull. Chem. Soc. Jap.* 1992, **65**, 1006–1011.

51. N. C. Bruno, S. L. Buchwald. *Org. Lett.*, 2013, **15**, 2876–2879.

Figure Captions

(a) Pd(II) complexes of 4,5-dimethyl-/diethyl-imidazolyl- (**dm** / **de**) ligand series

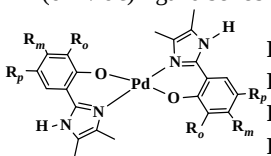

Pd(R~dm)$_2$ series

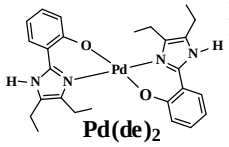

Pd(de)$_2$

Pd Complexes	R_o	R_m	R_p
Pd(*o*-*t*Bu~dm)$_2$	*t*Bu	H	H
Pd(*p*-*t*Bu~dm)$_2$	H	H	*t*Bu
Pd(*o*-M~dm)$_2$	OMe	H	H
Pd(*p*-M~dm)$_2$	H	H	OMe
Pd(*p*-Br~dm)$_2$	H	H	Br
Pd(*p*-N~dm)$_2$	H	H	NO_2

(b) Pd(II) complexes of 4,5-diphenyl-imidazolyl- (**dp**) ligand series

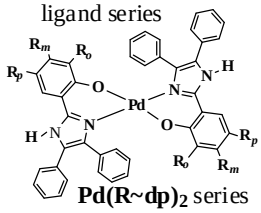

Pd(R~dp)$_2$ series

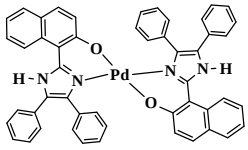

Pd(Naph~dp)$_2$

Pd Complexes	R_o	R_m	R_p
Pd(*o*-*t*Bu~dp)$_2$	*t*Bu	H	H
Pd(*p*-*t*Bu~dp)$_2$	H	H	*t*Bu
Pd(dp)$_2$	H	H	H
Pd(*o*-H~dp)$_2$	OH	H	H
Pd(*m*-H~dp)$_2$	H	OH	H
Pd(*p*-H~dp)$_2$	H	H	OH
Pd(*o*-M~dp)$_2$	OMe	H	H
Pd(*m*-M~dp)$_2$	H	OMe	H
Pd(*p*-M~dp)$_2$	H	H	OMe
Pd(*p*-Br~dp)$_2$	H	H	Br
Pd(*p*-N~dp)$_2$	H	H	NO_2

(c) Complexes of rigid / bulky ligand analogues

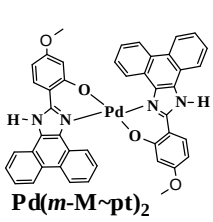

Pd(*m*-M~pt)$_2$

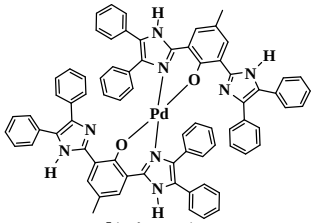

Pd(Bis-Im)$_2$

(d) An example of preparation for the Pd(II) complexes

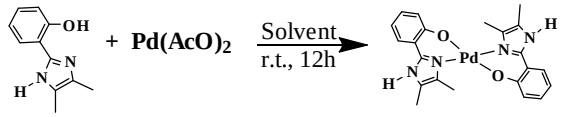

Scheme 1: (a) – (c) Palladium complexes employed in this study and **(d)** general synthetic scheme for the palladium complexes; ligand abbreviations have been chosen to reflect the phenol ring and the 4,5-imidazole substituents

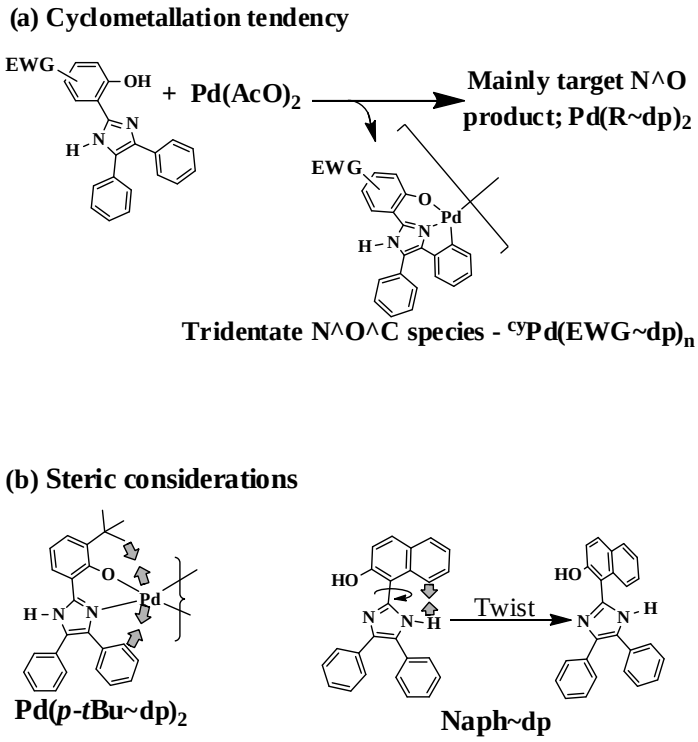

Scheme 2: (a) Formation of Pd–C organometallic species by 2-(4,5-diphenyl-1H-imidazol-2-yl)phenol derivatives apparently aided by electron withdrawing functions on phenol ring and **(b)** steric implications for *t*-Bu-, Ph- and naphtholyl- moieties.

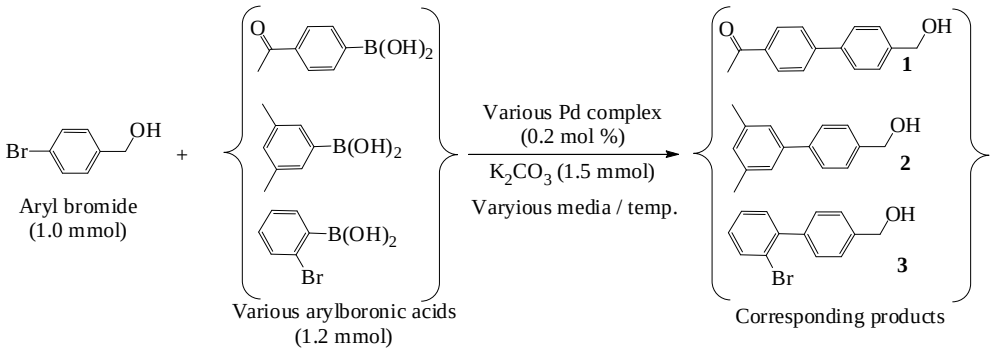

Scheme 3: Cross-coupling reactions carried out.

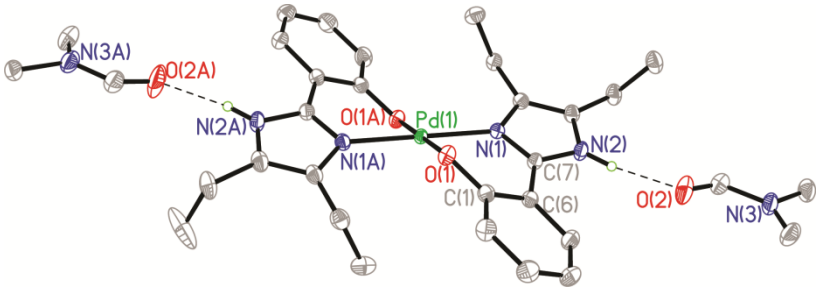

Fig. 1: Molecular structure of **Pd(de)$_2$***2dmf with thermal ellipsoids drawn at the 50 % probability level. Some atomic labels and protons have been omitted for clarity.

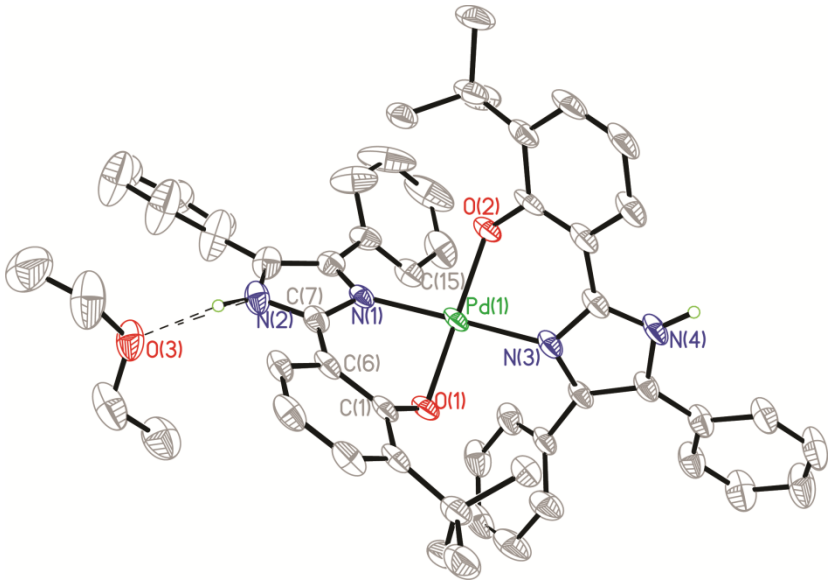

Fig. 2: Molecular structure of **Pd(*o*-*t*Bu~dp)$_2$***Et_2O with thermal ellipsoids drawn at the 50 % probability level. Some atomic labels and protons have been omitted for clarity.

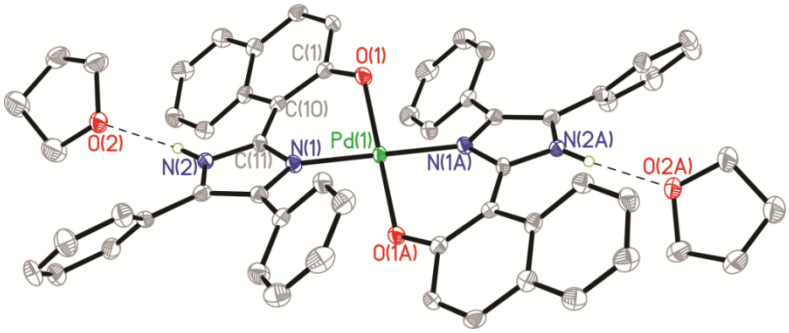

Fig. 3: Molecular structure of **Pd(Naph~dp)$_2$***2thf with thermal ellipsoids drawn at the 50 % probability level. Some atomic labels and protons have been omitted for clarity.

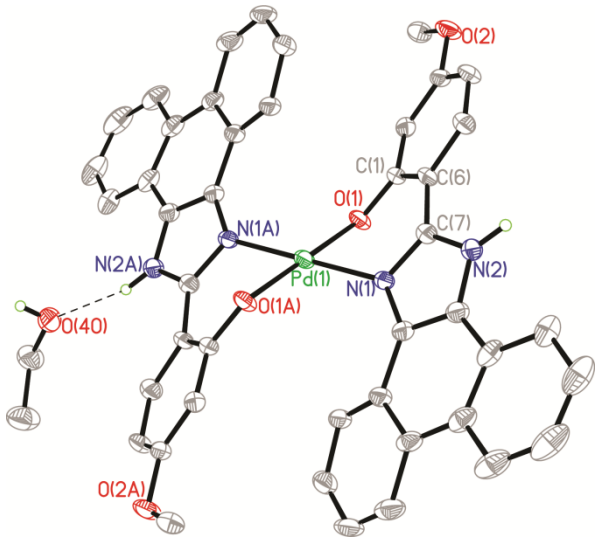

Fig. 4: Molecular structure of **Pd(*m*-M~pt)$_2$***EtOH with thermal ellipsoids drawn at the 50 % probability level. Some atomic labels and protons have been omitted for clarity.

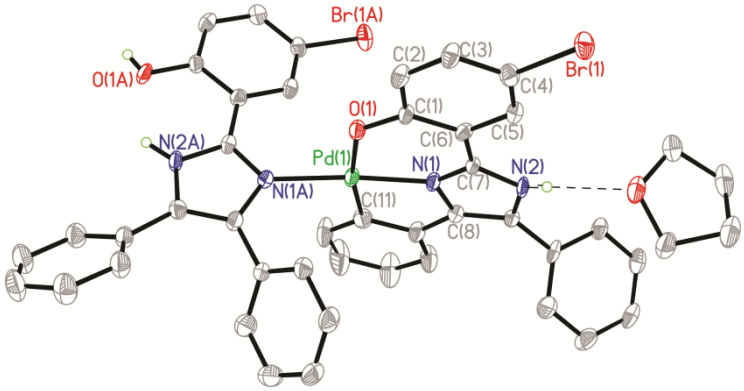

Fig. 5: Molecular structure of ^{cy}**Pd(*p*-Br~dp)$_2$** with thermal ellipsoids drawn at the 50 % probability level. Some atomic labels and protons have been omitted for clarity. Some atomic labels and protons have been omitted for clarity.

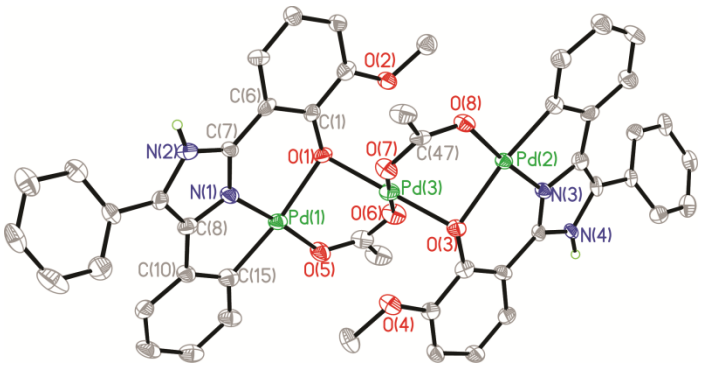

Fig. 6: Molecular structure of ^{cy}**Pd$_3$(*o*-M~dp.AcO)$_2$** with thermal ellipsoids drawn at the 50 % probability level. Some atomic labels and protons have been omitted for clarity.

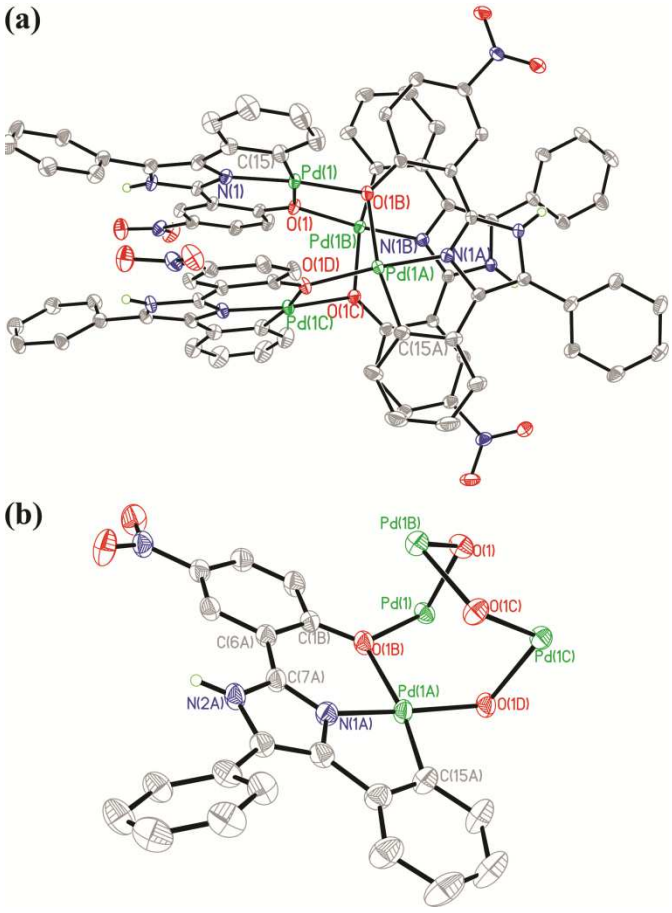

Fig. 7: **(a)** Molecular structure of ^{cy}**Pd$_4$(*p*-N~dp)$_4$** and **(b)** its tetranuclear metal center coordination framework. Thermal ellipsoids are drawn at the 50 % probability level and some atomic labels, protons and parts of some ligands in **(b)** have been omitted for clarity.

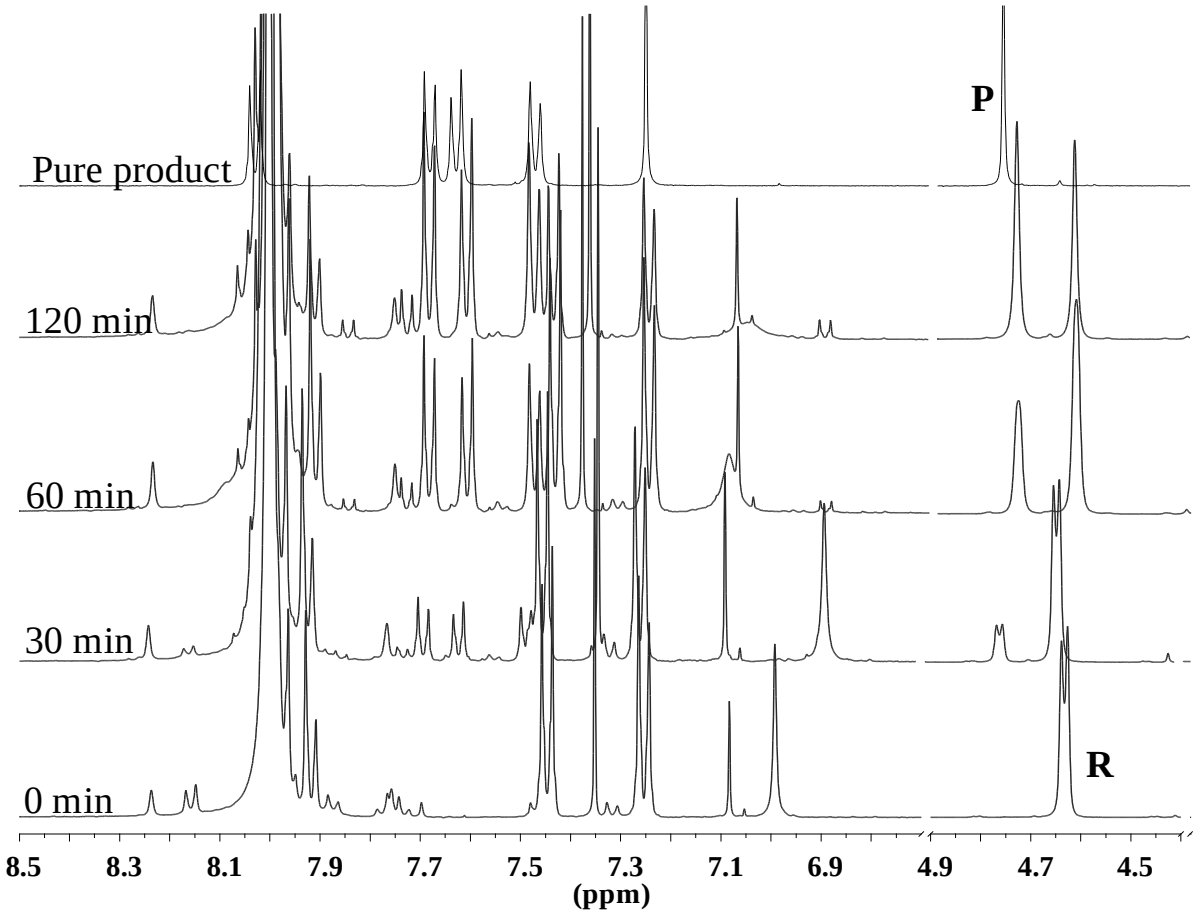

Fig. 8: Spectral stack for NMR experiments obtained during catalysis runs using 0.2 mol % **Pd(de)$_2$** at 100 ^{o}C in 3 mL dmf / 1 mL H_2O. The region of the methylene signals is separated and the corresponding reactant and product methylene peaks are denoted as **R** and **P**, respectively.

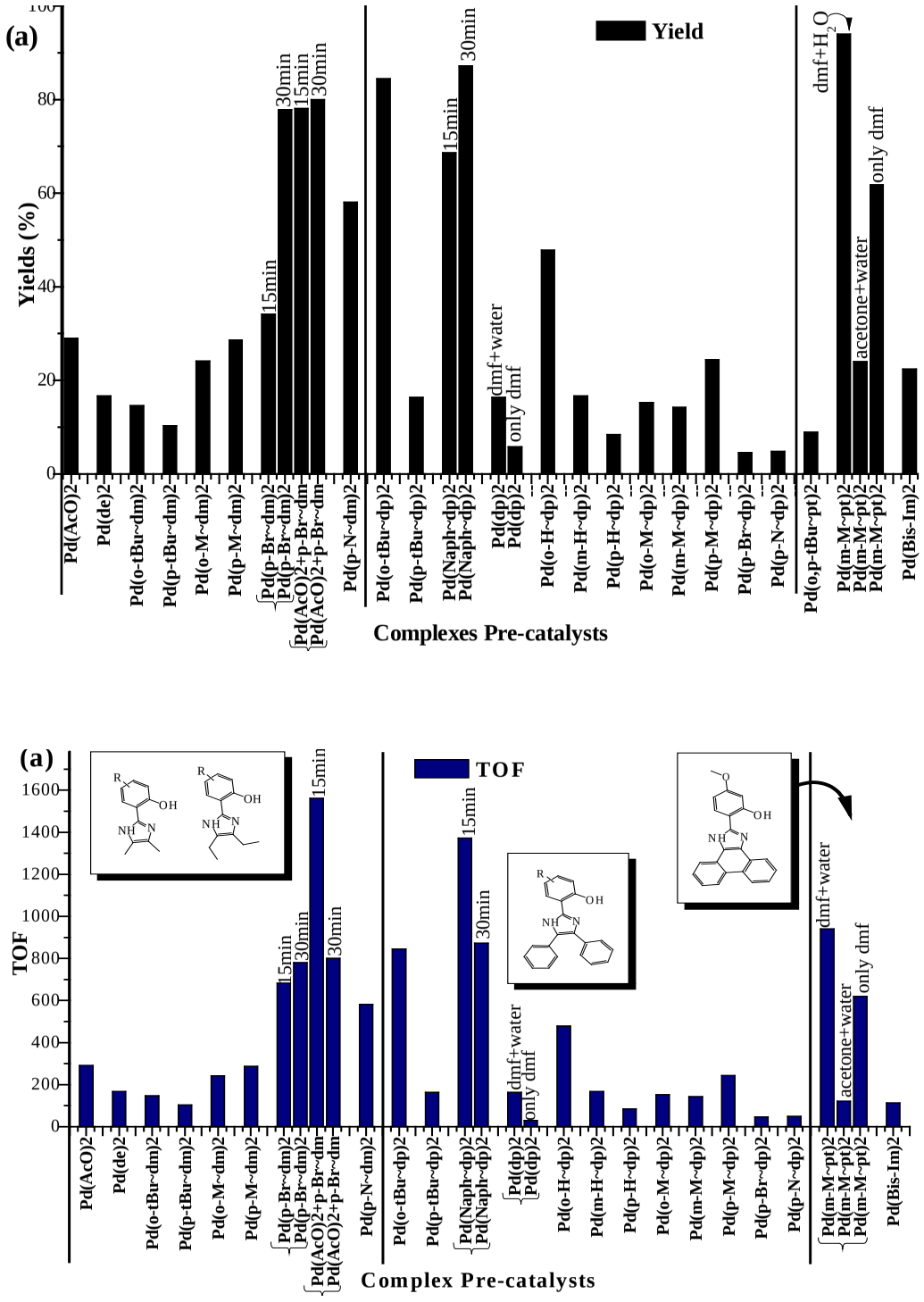

Fig. 9: Bar chart representing **(a)** catalytic yields and **(b)** catalytic turnover frequencies of the palladium pre-catalysts

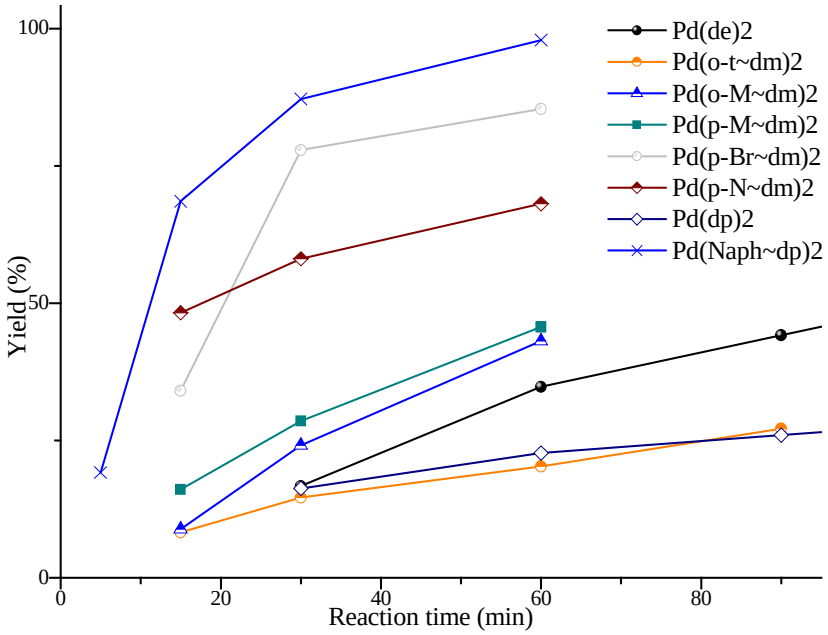

Fig. 10: Plot of reaction yield against reflux duration for catalysis experiments catalyzed by selected palladium pre-catalysts.

Tables

Table 1: Crystal data processing parameters for complexes **Pd.de**, **Pd.*o*-*t*Bu~dp**, **Pd(Naph~dp)$_2$** and **Pd.*m*-M~pt**.

	Pd.de*2dmf	**Pd.*o*-*t*Bu~dp***Et_2O	**Pd(Naph~dp)$_2$***2thf	**Pd.*m*-M~pt***EtOH
Formula	$C_{32}H_{46}N_6O_4Pd$	$C_{58}H_{66}N_4O_{4.5}0Pd$	$C_{66}H_{66}N_4O_6Pd$	$C_{48}H_{42}N_4O_6Pd$
Formula weight	685.15	997.55	1117.63	877.26
Temperature (K)	133(2)	133(2)	133(2)	133(2)
Wavelength (Å)	0.71073	0.71073	0.71073	0.71073
Crystal system	Monoclinic	triclinic	Monoclinic	Monoclinic
space group	P2(1)/c	P-1	P2(1)/n	P2(1)/c
a (Å)	12.6497(2)	12.4900(4)	10.3873(3)	11.2809(3)
b (Å)	19.2920(4)	15.0982(5)	18.5775(4)	11.0976(3)
c (Å)	14.2750(3)	16.1407(6)	14.0122(4)	15.3994(4)
α (deg)	90	89.817(2)	90	90
β (deg)	110.8580(10)	70.014(1)	97.6190(10)	92.0710(10)
γ (deg)	90	76.435(2)	90	90
Volume (Å^3)	3255.34(11)	2770.77(16	2680.06(12)	1926.61(9)
Z	4	2	2	2
Calculated density (g·m^{-3})	1.398	1.196	1.385	1.512
μ (mm^{-1})	0.615	0.382	0.405	0.541
F(000)	1432	1048	1168	904
Crystal size (mm)	0.05×0.05×0.05	0.06×0.05×0.04	0.06×0.05×0.04	0.08× 0.06×0.05
θ range (deg)	2.73–28.06	2.90–27.53	2.83–27.46	2.65–27.18
Limiting indicates	–16 ≤ h ≤ 16 –25 ≤ k ≤ 25 –18 ≤ l ≤ 18	–14 ≤ h ≤ 16 –19 ≤ k ≤ 18 –20 ≤ l ≤ 20	–13 ≤ h ≤ 13 –24 ≤ k ≤ 23 –18 ≤ l ≤ 18	–14 ≤ h ≤ 14 –13 ≤ k ≤ 13 –18 ≤ l ≤ 19
No. of rflns collected	39506	17976	11274	11064
No. of unique rflns	7599	12309	6072	3752
R(int)	0.0211	0.0323	0.0454	0.0305
Completeness to *θ* (%)	96.2 % (*θ*=28.06)	96.20 % (*θ*=27.53)	99.1 % (*θ*=27.46)	87.5 % (*θ*=27.18)
No. of parameters	444	592	335	271
Goodness-of-fit on F^2	0.992	1.109	1.044	1.022
Final R indices (I>2sigma(I))	R1 = 0.0227 wR2 = 0.0622	R1 = 0.0833 wR2 = 0.2280	R1 = 0.0537 wR2 = 0.1063	R1 = 0.0393 wR2 = 0.1056
R indices (all data)	R1 = 0.0267 wR2 = 0.0654	R1 = 0.0931 wR2 = 0.2379	R1 = 0.0718 wR2 = 0.1163	R1 = 0.0577 wR2 = 0.1173
Largest diff. peak and hole (e Å^{-3})	0.547, –0.460	2.216, –1.769	0.714, –0.659	0.898, –0.882

Table 2: Crystal data processing parameters for the cyclometallated palladium species ^{cy}**Pd(*p*-Br~dp)$_2$**, ^{cy}**Pd$_3$(*o*-M~dp.AcO)$_2$** and ^{cy}**Pd$_4$(*p*-N~dp)$_4$**.

	^{cy}**Pd(*p*-Br~dp)$_2$**	^{cy}**Pd$_3$(*o*-M~dp.AcO)$_2$**	^{cy}**Pd$_4$(*p*-N~dp)$_4$**
Formula	$C_{50}H_{44}Br_2N_4O_4Pd$	$C_{52}H_{46}N_4O_{12}Pd_3$	$C_{100}H_{88}N_{12}O_{26}Pd_4$
Formula weight	1031.11	1238.13	2299.42
Temperature (K)	133(2)	133(2)	133(2)
Wavelength (Å)	0.71073	0.71073	0.71073
Crystal system	Triclinic	Monoclinic	Tetragonal
space group	P-1	P2(1)	I4(1)/a
a (Å)	12.6804(3)	12.6040(5)	21.8632(4)
b (Å)	13.9288(3)	14.6747(6)	21.8632(4)
c (Å)	14.6994(2)	13.9666(6)	21.5503(5)
α (deg)	111.950(1)	90	90
β (deg)	114.268(1)	106.946(2)	90
γ (deg)	91.254(1)	90	90
Volume (Å^3)	2147.44(7)	2471.09(18)	10301.0(4)
Z	2	2	4
Calculated density (g·m^{-3})	1.595	1.664	1.483
μ (mm^{-1})	2.344	1.147	0.766
F(000)	1040	1240	4656
Crystal size (mm)	0.05 × 0.05 × 0.04	0.07 × 0.07 × 0.04	0.06 × 0.05 × 0.04
θ range (deg)	3.60–27.52	2.78–32.48	2.95–28.04
Limiting indicates	$-16 \le h \le 16$	$-17 \le h \le 18$	$-24 \le h \le 26$
	$-18 \le k \le 17$	$-12 \le k \le 21$	$-20 \le k \le 28$
	$-19 \le l \le 19$	$-16 \le l \le 20$	$-25 \le l \le 25$
No. of rflns collected	14382	24473	11274
No. of unique rflns	9682	10955	6072
R(int)	0.0319	0.0502	0.0454
Completeness to θ (%)	97.90 % (θ=27.52)	85.95 % (θ=32.48)	99.10 % (θ=27.46)
No. of parameters	582	636	353
Goodness-of-fit on F^2	1.139	1.018	1.044
Final R indices (I>2sigma(I))	R1 = 0.0538	R1 = 0.0534	R1 = 0.0537
	wR2 = 0.1084	wR2 = 0.1258	wR2 = 0.1063
R indices (all data)	R1 = 0.0718	R1 = 0.0864	R1 = 0.0718
	wR2 = 0.1195	wR2 = 0.1450	wR2 = 0.1163
Largest diff. peak and hole (e Å^{-3})	1.179 –0.763	1.880, –1.961	0.714, –0.659

Table 3: Selected structural data

Properties / Complexes	Pd1–O1 (Å)	Pd1–N1 (Å)	Pd1–C1 (Å)	C1–O1 (Å)	C1-C6-C7-N1[a] Torsion (°)
Pd(de)$_2$	1.9934(17)	2.0321(13)	NA	1.3257(18)	21.933(253)
Pd(*o*-*t*Bu~dp)$_2$	2.0210(40)	2.0040(40)	NA	1.3340(60)	31.912(873)
Pd(Naph~dp)$_2$	1.9868(23)	2.0009(21)	NA	1.3210(40)	21.454(458)
Pd(*m*-M~pt)$_2$	2.0274(21)	2.0135(23)	NA	1.3430(40)	19.022(499)
^{cy}Pd(*p*-Br~dp)$_2$	2.1300(30)	1.9530(40)	1.9920(50)	1.3340(50)	2.787(816)
^{cy}Pd$_3$(*o*-M~dp.AcO)$_2$	2.1360(50)	1.9280(70)	1.9640(80)	1.3400(90)	4.615(121)
^{cy}Pd$_4$(*p*-N~dp)$_4$	2.0710(30)	1.9320(30)	1.9680(40)	1.3280(50)	4.267(615)

[a]The corresponding atoms C6 and C7 for **Pd(Naph~dp)$_2$** are actually C10 and C11 respectively.

Table 4: Results for catalytic performance by 0.2 mol. % of **Pd.de$_2$** under varying reaction conditions

Entry	Rxn time (min)	Base (1.5 mmol)	Temp. (^{o}C)	Media	Yield (%)
1	30	K_2CO_3	153	3EtOH:1H_2O	5.9[a]
2	"	None	"	"	Trace
3	120	K_2CO_3	"	3Acetone:1H_2O	3.7
4	60	"	"	dmf	Trace
5	120	"	80	3dmf:1H_2O	2.6
6	30	"	100	"	16.7
7	60	"	"	"	34.8
8	120	"	"	"	53.5

Table 5: Catalytic performance for the series of Pd compounds.[a]

Entry	Complex	Media	Time (min)	Temp. (^oC)	Yield[b] (%)	TOF (h^{-1})
1	$Pd(AcO)_2$	3dmf:1H_2O	30	100	29.0	290
2	$Pd(de)_2$	3dmf:1H_2O	30	100	16.7	167
3	Pd(*o*-*t*Bu~dm)$_2$	"	30	"	14.6	146
4	Pd(*p*-*t*Bu~dm)$_2$	"	30	"	10.3	103
5	Pd(*o*-M~dm)$_2$	"	30	"	24.1	241
6	Pd(*p*-M~dm)$_2$	"	30	"	28.6	286
7i	Pd(*p*-Br~dm)$_2$	"	15	"	34.1	682
7ii	Pd(*p*-Br~dm)$_2$	"	30	"	77.9	779
8i[46]	$Pd(AcO)_2$+*p*-Br~dm	"	15	"	78.1	1562
8ii[46]	$Pd(AcO)_2$+*p*-Br~dm	"	30	"	80.0	800
9	Pd(*p*-N~dm)$_2$	"	30	"	69.0	690
10	Pd(*o*-*t*Bu~dp)$_2$	3dmf:1H_2O	30	100	84.5	845
11	Pd(*p*-*t*Bu~dp)$_2$	"	30	"	16.3	163
12i	Pd(Naph~dp)$_2$	"	15	"	68.6	1372
12ii	Pd(Naph~dp)$_2$	"	30	"	87.2	872
13i	$Pd(dp)_2$	"	30	"	16.3	163
13ii	$Pd(dp)_2$	dmf	120	153	5.8	14.5
14	Pd(*o*-H~dp)$_2$	3dmf:1H_2O	30	100	47.8	478
15	Pd(*m*-H~dp)$_2$	"	30	"	16.7	167
16	Pd(*p*-H~dp)$_2$	"	30	"	8.4	84
17	Pd(*o*-M~dp)$_2$	"	30	"	15.2	152
18	Pd(*m*-M~dp)$_2$	"	30	"	14.2	142
19	Pd(*p*-M~dp)$_2$	"	30	"	24.4	244
20	Pd(*p*-Br~dp)$_2$	"	30	"	4.6	46
21	Pd(*p*-N~dp)$_2$	"	30	"	4.8	48
22i	Pd(*m*-M~pt)$_2$	3dmf:1H_2O	30	100	**94.0**	**940**
22ii	Pd(*m*-M~pt)$_2$	3Acetone:1H_2O	120	60	24.0	60
22iii	Pd(*m*-M~pt)$_2$	dmf	30	153	61.8	619
23	Pd(Bis-Im)$_2$	dmf	120	153	22.4	56

[a]Reaction conditions: 1.2 mmol of (4-acetylphenyl)boronic acid; 1 mmol of (4-bromophenyl)methanol; palladium complex loading, 0.2 mol %; Solvent media, 4 mL of 3:1 solvent/H_2O mixture. [b]Yield determined by ^{1}H-NMR.

Table 6: Coupling of other boronic acid substrates using **Pd(Naph~dp)$_2$** at 100 ^{o}C and 30 min reaction time in 3:1 dmf/H_2O media.

Entry	Aryl-aryl coupling product	Time (min)	Yield (%)	TOF (h^{-1})
1	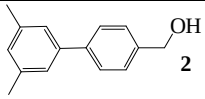 **2**	5	18.7	1122
		15	58.2	1164
2	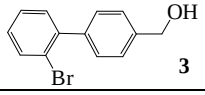 **3**	5	Trace	–
		15	Trace	–